THESIS FOR THE DEGREE OF DOCTOR OF PHILOSOPHY

# NORBORNADIENES FOR SOLAR THERMAL ENERGY STORAGE AND NEW APPLICATIONS

Design, Synthesis, Characterisation and Device Testing

AMBRA DREOS


CHALMERS

Department of Chemistry and Chemical Engineering

CHALMERS UNIVERSITY OF TECHNOLOGY

Gothenburg, Sweden, 2019

Norbornadienes for Solar Thermal Energy Storage and New Applications
Design, Synthesis, Characterisation and Device Testing
AMBRA DREOS
ISBN 978-91-7597-859-8



Doktorsavhandlingar vid Chalmers tekniska högskola
Ny serie nr. 4540
ISSN 0346-718X

Department of Chemistry and Chemical Engineering
Chalmers University of Technology
SE-41296 Göteborg
Sweden
Telephone +46 (0)31-7721000

Cover: Envisioning a closed cycle solar thermal energy storage technology based on liquid norbornadienes. Adapted with permission from the illustration by Katja Mock for the cover illustration of Advanced Energy Materials, Volume 8, Issue 18, June 2018.

Chalmers Reproservice
Gothenburg, Sweden 2019.

# Abstract

NORBORNADIENES FOR SOLAR THERMAL ENERGY STORAGE AND NEW APPLICATIONS

Design, Synthesis, Characterisation and Device Testing

Ambra Dreos
Department of Chemistry and Chemical Engineering
Chalmers University of Technology

The energy demand worldwide is steadily increasing, therefore it is fundamental to efficiently utilise renewable energy resources. Energy storage technologies are particularly relevant in order to be able to exploit renewable energy resources such as solar energy, since these are typically intermittent and not evenly distributed. The work presented in this thesis is focused on trying to optimise norbornadiene-quadricyclane systems to harness and store solar energy. Norbornadienes are able to absorb light, and undergo photoinduced isomerization to the high energy isomer quadricyclane, which is stable over time. When quadricyclanes back isomerise to norbornadienes they release the absorbed energy as heat. This technology is called “molecular solar thermal”, or MOST. Different features need to be optimised in order to utilise norbornadiene-quadricyclane photoswitches for MOST applications. In my work I focused on synthesising new norbornadienes, characterising their molecular and spectroscopic properties, and trying to optimise them for energy storage purposes. In particular I focused on identifying specific structure-properties relationship that allow selectively engineering the kinetic stability of quadricyclanes, to achieve longer storage times. This was in fact achieved in a series of norbornadienes by selectively increasing the entropy of activation to the back isomerization. A small device was also built, in order to test a hybrid technology that would combine MOST and solar water heating. These laboratory-scale experiments were particularly instructive in demonstrating the potential of MOST systems, and learning about the future challenges. Liquid, neat norbornadienes were also made, and their properties assessed. They retained the ability to photoisomerise and back convert in neat samples, but new challenges arose, such as stability over multiple cycles and storage times. Moreover, the use of a norbornadiene-quadriyclane photoswitch as a molecular keypad lock is demonstrated.

Keywords: Solar energy; energy conversion; thermal energy storage; molecular switches; norbornadiene; quadricyclane; molecular logic; molecula keypad locks

# Acknowledgements

I would like to acknowledge my supervisor Kasper Moth-Poulsen for trusting me to investigate this project. Thank you for guiding me with optimism and calm even in the harder moments, it made me considerably grow on a professional level. I deeply appreciate the kind support, freedom and independence that you let me have in these years. Not everyone is lucky enough to be allowed to pursue their own interests within the projects. It has been a great experience that taught me to be a more independent researcher. Thanks to co-supervisor Karl Börjesson for the always on point scientific supervision every time it was needed. Your practical attitude and sharp mind have been fundamental in shaping me as a researcher. Thanks to co-supervisor Maria Abrahamsson for the mentoring on the upconversion project (and much more) during the last year. These results unfortunately did not make it in this thesis, but are for me a precious experience. The funding agencies (SSF and Wallenberg) and Chalmers are acknowledged for making this research possible. I am very grateful to my many collaborators, it has been a great pleasure to work with you. K. Jorner, V. Gray, J. Andréasson, not only we shared some fun science, but I learnt a great deal from working with you. Thanks to M. Mayzel for the support with the NMR experiments at the Swedish NMR Centre. Thanks to the MOST team over the years, and especially to Z. Wang and M. Quant for the fruitful collaborations. Also thanks to B. E. Tebikachev, H. Ottosson, J. Udmark, M. B. Nielsen, P. Erhart, A. Ström, E. Sundén, J. Mårtensson, B. Kücüköz, and all the people that helped with their time and knowledge when it was needed. To the nice colleagues on floor 8 and beyond, thank you for sharing the everyday struggles, coffees and fun times. Especially thanks to Lotta for taking care of us everyday and making this place a special one.

My dear friends, adventures companions, and family, I am grateful everyday for having you in my life, and this work would definitely not have been possible without every one of you.

# List of Publications

The thesis consists of an introduction, summary, and discussion of the results presented in the following appended papers:

| | |
|---|---|
| **Paper I** | **Liquid Norbornadiene Photoswitches for Solar Energy Storage**, Dreos A., Wang Z., Udmark J., Ström A., Erhart P., Börjesson K., Moth-Poulsen K. *Advanced Energy Materials,* 2018, **8**, 170341. |
| **Paper II** | **Unraveling Factors Leading to Efficient Norbornadiene-Quadricyclane Molecular Solar-Thermal Energy Storage Systems**, Jorner K., Dreos A., Emanuelsson R., El Bakouri O., Galvan I. F., Börjesson K., Feixas F., Lindh R., Zietz B., Moth-Poulsen K., Ottosson H., *Journal of Materials Chemistry A*, 2017, **5**, 12369-12378 |
| **Paper III** | **Exploring the Potential of a Hybrid Device Combining Solar Water Heating and Molecular Solar Thermal Energy Storage**, Dreos A., Börjesson K., Wang Z., Roffey A., Norwood Z., Kushnir D., Moth-Poulsen K., *Energy and Environmental Science*, 2017, **10**, 728-734. |
| **Paper IV** | **A three-input molecular keypad lock based on a norbornadiene-quadricyclane photoswitch**, Dreos A., Wang Z., Tebikachew B. E., Moth-Poulsen K., Andréasson J., Journal of Physical Chemistry Letters, 2018, **9**, 6174-6178. |

The following published papers are not included in the thesis:

| | |
|---|---|
| **Paper A** | **Low molecular weight norbornadiene derivatives for molecular solar-thermal energy storages**, Quant M., Lennartson A., Dreos A., Kuisma M., Erhart P., Börjesson K., Moth-Poulsen K., *Chemistry - A European Journal*, 2016, **22**, 13265-13274 |
| **Paper B** | **Loss channels in Triplet-Triplet Annihilation Photon Upconversion: Importance of Annihilator Singlet and Triplet Surface Shapes**, Gray V., Dreos A., Erhart P., Albinsson B., Moth-Poulsen K., Abrahamsson M., *Physical Chemistry Chemical Physics*, 2017, **19**, 10931-10939. |
| **Paper C** | **Macroscopic Heat Release in a Molecular Solar Thermal Energy Storage System**, Wang Z., Roffey A., Losantos R. Lennartson A., Jevric M., Petersen A. U., Quant M., Dreos A., Wen X., Sampedro D., Börjesson K., Moth-Poulsen K., *Energy and Environmental Science,* DOI: 10.1039/C8EE01011K |
| **Paper D** | **Norbornadiene-based photoswitches with exceptional combination of solar spectrum match and long term energy storage**, Jevric M., Petersen A. U., Mansoe M., Singh S. K., Wang Z., Dreos A., Sumby C., Nielsen M. B., Börjesson K., Erhart P., Moth-Poulsen K., *Chemistry - A European Journal,* 2018, **24**, 12767-12772. |

# CONTRIBUTION REPORT

| | |
|---|---|
| **Paper I** | Designed and synthesized most of the compounds (J. Udmark contributed to the synthesis of some of them). Performed all the characterisation, except theoretical calculations. Sheer viscosity was measured together with A. Ström. Wrote most of the manuscript, with inputs from other authors. |
| **Paper II** | Performed the kinetic characterisation, DSC, NMR study, built the device and done the device test. Wrote parts of the manuscript on the performed work. |
| **Paper III** | Participated in the design of the device, built the device, performed all the experiments, except the device simulation and the cyclability experiment. Wrote the manuscript together with the other authors. |
| **Paper IV** | Developed the idea for the project, performed all the experiments except for the characterisation of the quadricyclane to norbornadiene photoisomerization and cyclability test, wrote the manuscript together with other authors. |

# Contents

# List of Abbreviations

| | |
|---|---|
| MOST | Molecular solar thermal |
| $\triangle H_{storage}$ | Energy storage |
| $\triangle G^{\ddagger}$ | Free energy energy of activation |
| $\phi$ | Photoisomerization quantum yield |
| $n_{converted}$ | Number of isomerised molecules |
| $n_{photons}$ | Number of absorbed photons |
| $\triangle H^{\ddagger}$ | Enthalpy of activation |
| $t_{1/2}$ | Half life |
| NBD | Norbornadiene |
| QC | Quadricyclane |
| UV | Ultraviolet |
| Vis | Visible |
| $A_{onset}$ | Absorption onset |
| $A$ | Absorbance |
| $I_0$ | Intensity of incident light |
| $I$ | Intensity of the transmitted light |
| $T$ | Transmittance |
| $\varepsilon$ | Molar absorptivity |
| $l$ | Path length |
| $c$ | Concentration |
| $k$ | Rate constant |
| $T$ | Temperature |
| $\triangle S^{\ddagger}$ | Entropy of activation |
| $R$ | Gas constant |
| $h$ | Planck´s constant |
| $I$ | photon flux |
| $N_A$ | Avogadro´s number |

| | |
|---|---|
| $V$ | Volume |
| $\beta$ | Fraction of absorbed photons |
| $h\nu$ | Light |
| $\Delta$ | Heat |
| EDG | Electron donating group |
| EWD | Electron withdrawing group |
| NMR | Nuclear magnetic resonance |
| VT | Variable temperature |
| NOESY | Nuclear Overhouser effect spectroscopy |
| NOE | Nuclear Overhauser effect |
| DSC | Differential scanning calorimetry |
| D-A | Diels-Alder |
| Me | Methyl |
| iPr | Isopropyl |
| SWH | Solar water heating |
| PTFE | Polytetrafluoroethylene |
| $\eta_{MOST}$ | Solar energy storage efficiency |
| $\alpha$ | Conversion fraction |
| $\dot{\eta}_{MOST}$ | MOST flow speed |
| $A$ | Irradiated surface |
| $E_{AM1.5}$ | Energy of incoming radiation, calibrated to the AM 1.5 solar standard |
| $\eta_{SWH}$ | Solar water heating efficiency |
| $\dot{m}_{H_2O}$ | Water flow rate |
| $C_{PH_2O}$ | Water heat capacity |
| $\triangle T$ | Temperature increase |

# Chapter 1

# Introduction

The average temperature on Earth has been significantly increasing in the last 200 years, which is now attributed mainly to the impact of human induced emissions of greenhouse gasses.[1] Profound changes in the climate have been observed worldwide, and widespread effects are predicted to transform the global environment.

In 2016, 196 country representatives met in Paris to discuss the climate change Paris agreement, which is one of the first global efforts to set common objectives in order to contrast climate change. In this agreement one of the main goal is to maintain the global average temperature below 2℃ above pre-industrial levels, with focus also put on the systemic changes necessary to achieve it.[2] While an important milestone, the Paris agreement was also received with criticism because it does not agree on specific plans, it is voluntary and not enforced and, according to many, not enough is in fact happening to ensure that the defined goals will be respected.[3–5]

Energy generation and industry are responsible for about 65% of the emitted green house gasses, therefore the energy sector needs to be re-thinked in order to respect the 2℃ target.[6] In IRENA global energy roadmap "REmap", it is shown how, while today 84% of the used energy come from fossil fuels, 65% of the energy could actually realistically come from renewables past 2015.[7] This achievement, together with energy efficiency, would allow respecting of the 2℃ goal as set in the Paris agreement, by meeting about 90% of the needed decarbonisation.

Solar and wind energy could play a key role in the future energy landscape due to their tremendous potential.

The sun irradiation has a lot of energy, as can be seen in Figure 1.1. Even in

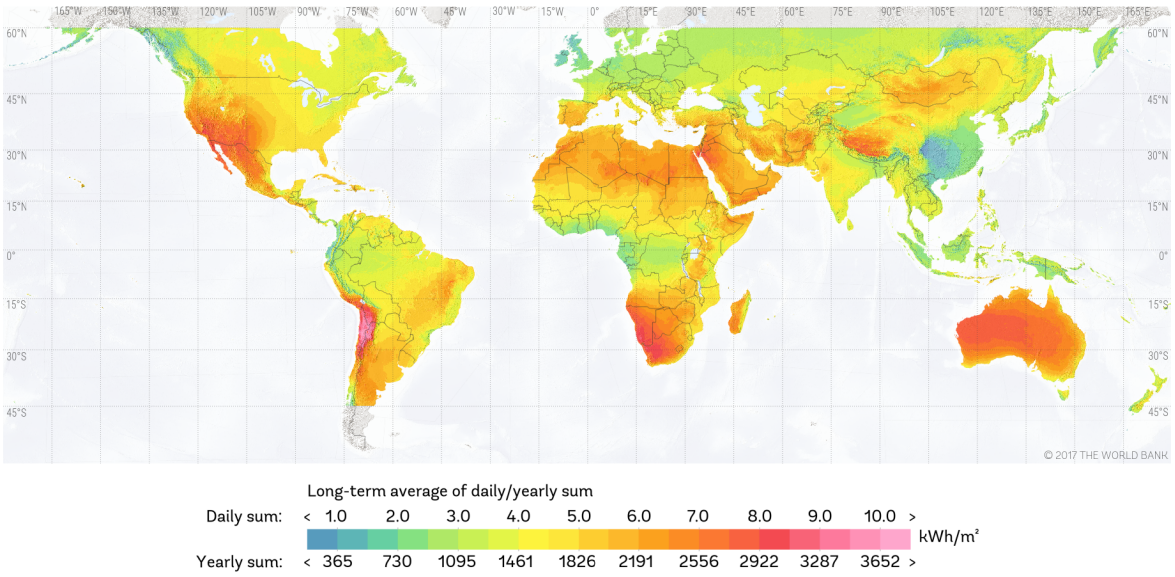


**Figure 1.1:** World map of Direct Normal Irradiation, a parameter showing the potential of solar energy when collected by tilted or sun-tracking photovoltaic modules. © 2017 The World Bank, Solar resource data: Solargis.

Sweden, where the sun radiation is not at its peak, there is at least about 1000 kWh/m$^2$ that could be potentially collected over a year. To put this value into context, in Sweden, in 2014, 13000 kWh of electric power has been consumed per capita, which means that 13 m$^2$ would be enough to supply the yearly electric power needed for one person.[8]

Utilising the sun radiation is not an easy challenge; it requires new efficient harvesting technologies, and adapting the energy grid to them. A lot of research is nowadays being invested toward new technologies for harvesting, storage and utilisation of solar energy. Some fields that have seen promising advances are photovoltaic (harnessing of solar light to provide electricity),[9–13] artificial photosynthesis (harnessing of solar light to provide fuels which store the solar energy)[14,15] and solar thermal (harnessing and storing thermal energy).[16,17]

Integrating storage solutions in the energy grid can increase its flexibility and stability, improving access and utilisation of variable renewables and helping matching supply and demand. While some storing technologies are already being demonstrated and commercialised (such as batteries, underground thermal energy storage, or residential hot water storage), many are still being researched at early stages (such as thermochemicals, supercapacitors and others).[18] Since emerging storage technologies can play such a crucial role in the evolution of the global energy system toward decarbonisation, it is fundamental to keep investing in them in order to explore their full potential.

Energy storage technologies can be simply distinguished, based on their out-

come, in electrical or thermal. Thermal energy consist of about 50% of the total energy consumption, with 55% of it used in industry and agriculture, and 45% for domestic use.[19] Thermal energy is nowadays mainly obtained by fossil fuels, and partially from electrical energy.[19] Obtaining thermal energy from renewables as solar will have a significant impact on reducing greenhouse gas emissions. Decoupling thermal and electrical energy and effectively utilising thermal energy storage solutions is also an advantage, since it allows for load levelling by relieving peaks of demand in electrical energy, and contributing to overall more efficient energy systems. This has been practically implemented, for example in France where thermal energy storage solutions contributed to reducing the winter peak electricity demand by about 5%.[18] Different heating storage technologies can be distinguished in terms, for example, of their location, efficiency, output temperature ranges, storing time ranges.[18]

The landscape of possible energy storage technologies is complex, and therefore it is not trivial to exploit the great potential value of emerging technologies. It is important to analyse the existing market to understand what are the available technologies, and where there is potential for new applications. With new technologies being constantly researched and developed it is important for agencies and policy makers to keep an eye on the development of the energy storage field, and promote targeted actions to purposefully meet the energy system needs.

In the work presented in this thesis, a new energy storage technology is being investigated and developed. This technology is based on organic photoswitches; these are expected to absorb sun light, store it as chemical energy and to release the stored energy as heat on demand. The presented work covers a generic background explaining the concept, the molecular systems and the intrinsic limitations and challenges. Results on the molecular design, optimisation of the properties, and possible applications will be presented and discussed.

# Chapter 2

# Molecular Solar Thermal Energy Storage

*In this chapter the concept of Molecular Solar Thermal Energy storage is introduced and explained. Diferent molecular system that have been considered as MOST in the past are briefly presented, and norbornadiene-quadricyclane based MOST are introduced. Open challenges and some of the scientific questions behing the work presented in this thesis are defined.*

## 2.1 General Concept and Requirements

One energy storage concept is based on the exploitation of chemical systems which undergo photo induced processes, to store solar energy in form of chemical energy. The idea is to use compounds that upon exposure to light transform into high energy metastable species to harvest sun light and store its energy as chemical energy. The kinetically controlled thermal back conversion would then release the stored energy as heat. The thermal back conversion could be triggered by using heat or a catalyst, releasing the absorbed energy as heat on demand. This concept has been called “molecular solar thermal energy storage” (MOST) or “solar thermal fuels”.[20,21]

The key parameters defining the performance of a MOST system have been previously discussed,[22–24] and some of them are listed in Table 2.1. They can be divided in three main different categories: production and availability, photochemical and thermodynamic properties, and applications and materials. Specific key aspects are defined for each of these properties. Following is a general overview

**Table 2.1:** Some key properties of a MOST system.

| Production and Availability | Photochemical and Thermodynamic Properties | Applications and Materials |
|---|---|---|
| Starting materials | Solar spectrum match | Application |
| Synthesis | Spectral window | Physical state |
| Costs | Quantum yield | Cyclability |
| | Energy storage density | Heat release trigger |
| | Heat capacity | Materials safety |
| | High energy isomer half-life | Materials disposal |

of some of the properties and main concepts that define a MOST performance; these will be also discussed more in detail in the next chapters.

To be a competitive alternative to other thermal storage solutions on the market, MOST materials should be synthesised in simple and scalable ways from cheap starting materials, and the molecular properties of the chosen system should fulfil certain requirements. It is of course important for a MOST system to exhibit good solar spectrum match, by absorbing as much as possible light in the visible region. The high energy compound should not have an absorption spectrum overlapping with the parent compound. A spectral window between the two spectra is necessary to maximise the conversion of the parent compound, and to avoid the formation of a photostationary state. A relevant parameter is the quantum yield of the photo induced process. It is defined as:

$$\phi = \frac{n_{converted}}{n_{photons}} \tag{2.1}$$

with $n_{converted}$ the number of converted molecules, $n_{photons}$ the number of absorbed photons; an ideal MOST should have $\phi$ close to unity. The stored energy, expressed by $\Delta H_{storage}$, should be as high as possible, and the molecular weight as low as possible in order to ensure a high energy storage density. The heat capacity $C_P$ affects the observed temperature increase $\Delta T$ according to the following equation:

$$\Delta T = \frac{\Delta H_{storage}}{C_P} \tag{2.2}$$

therefore it needs to be as low as possible. The energy barrier of the back conversion should be sufficiently high, in order to ensure storage of the absorbed energy for extended periods of time with minimal discharge. In order to achieve high cyclability, both the photoconversion and back conversion processes should occur quantitatively with minimal degradation of the two compounds.

It is important to define the intended applications when developing a material. Daily or seasonal storage, medium or low heat would require MOST systems with very different properties in terms of energy storage times and density. The application would also dictate, for example, if a fast or slow heat release is needed; the use of a catalyst to trigger the back isomerization would allow fast release of the stored heat. Other challenges, as materials safety or disposal, are better evaluated at later stages.

## 2.2 Molecular Systems for MOST Applications

Different molecular systems which undergo photo induced processes have been investigated as MOST systems in the past.[22,24,25] These are usually photoswitches based on organic or organometallic compounds, which typically undergo isomerization or dimerisation as a consequence of absorption of light.

To understand how a hypothetical molecular system could be designed for this application, it is useful to describe a simplified energy diagram of a MOST system. As we can see in Figure 2.1, absorption of light induce the system to be in an excited state (simplified as $S_1$here). After relaxation, instead of converting back to the parent molecule, the system photoisomerise to a high energy isomer which is kinetically stable over some time. The high energy isomer eventually thermally rearranges to the parent compound, and release the stored energy as heat. From this scheme it is possible to correlate some of the above mentioned MOST properties to the specific molecular aspects determining them. The energy difference between the ground and excited state determine the absorption onset of the material. The probability of the photoisomerization to happen is expressed by the photoisomerization quantum yield (Equation 2.1). The energy difference between parent molecule and photoisomer correspond to the stored energy, and the activation energy for the thermal back isomerization will determine the energy storage time.

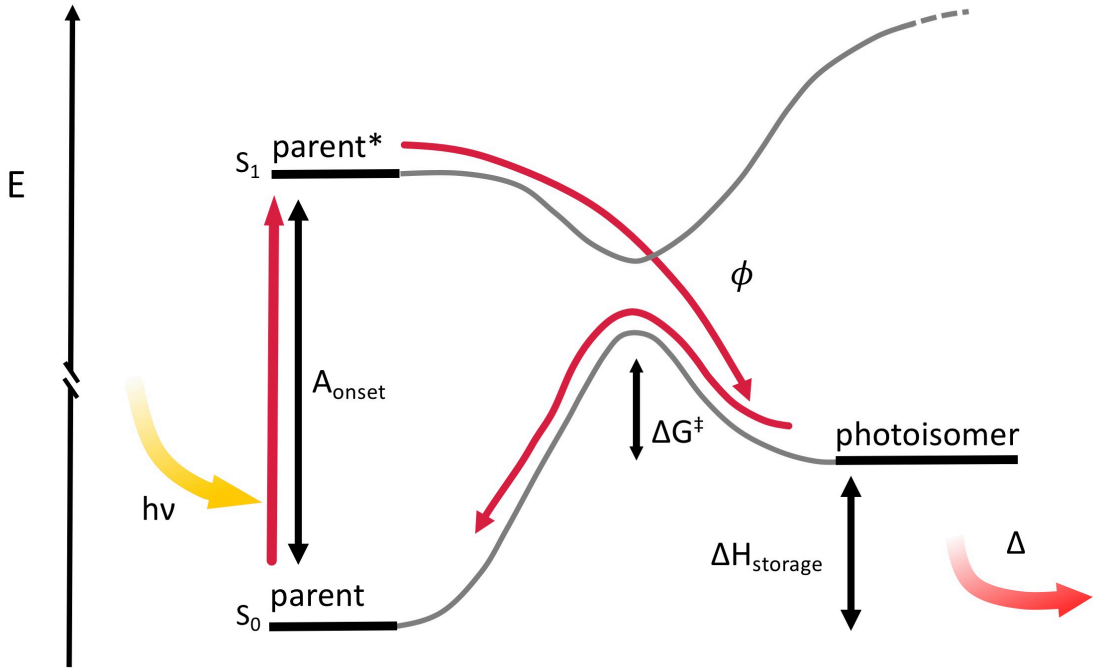


**Figure 2.1:** Energy scheme of a generic MOST system. Absorption of light, photo induced isomerization and thermal back conversion are indicated as red arrows. Some of the important parameters such as absorption onset ($A_{onset}$), energy storage ($\triangle H_{storage}$) and free energy of activation ($\triangle G^{\ddagger}$) are indicated as well.

Looking at the energy scheme in Figure 2.1 it is clear how all these properties are correlated, since they are different aspects of the same molecular system, which obey to basic physics laws. Eventual modifications are often limited and not independent, affecting multiple parameters at the same time. Discussions on the intrinsic limitations, and the potential of MOST technologies have been previously published.[25,26] It is important to notice how red-shifting the $A_{onset}$ has usually the effect of reducing $\triangle G^{\ddagger}$, and often also $\triangle H_{storage}$. Due to the non-crossing rule of electronic energy levels it is unrealistic to predict infinitely high $\triangle G^{\ddagger}$, and therefore the barrier for the back isomerization will have to be "paid" with part of the absorbed energy (at the end, there is no such thing as a "free lunch"). How much energy is needed, and for how long the energy needs to be stored, will therefore affect also how much it is realistic to red-shift the $A_{onset}$.

Börjesson *et al.* calculated the theoretical efficiency limit of an ideal MOST system, based on some assumptions.[26] For example, it was stated that an optimal MOST material should be liquid and solvent free (since addition of solvents would reduce the energy storage density). The parent molecule should be capable of absorbing all incoming photons below the absorption onset. In addition, this molecule should convert to a colourless photoisomer with $\phi$ as near

as possible as 100%. The solar energy conversion efficiency was then calculated assuming an energy barrier for the back isomerization (in this work defined equivalent to $\triangle H^{\ddagger}$ ) from 110 kJ/mol to 140 kJ/mol. These values would imply a half-life of the photoisomer, $t_{1/2}$, equal to 24 days at 25 ℃ or $4.3 \times 10^6$ days respectively. A $\triangle H^{\ddagger}$ parameter of 120 kJ/mol ($t_{1/2} = 1.4 \cdot 10^3$ days), could be a good value if seasonal storage applications were considered, and would yield a maximum calculated energy conversion efficiency between 10.6% and 12.4% with an absorption onset between 656 nm and 685 nm. It has been also previously stated that a MOST could be based on a compound with a molecular weight as low as 130 g/mol,[25] and it was then predicted that an overall optimised NBD could reasonably reach an energy storage density of 480 J/g. These values should give a good first indication of limitations and potential of a MOST technology, and should help to evaluate real molecular systems properties.

Organic and organometallic photoswitches have been considered in the past as MOST candidates. These molecular systems have often been modified, employing interesting chemical design approaches to engineer their properties and improve their performance as MOST. Some examples of studied systems include intramolecular dimerisation of anthracene and their derivatives,[27] $cis/trans$ isomerization of stilbenes,[28] $cis/trans$ isomerization of azobenzenes,[21,29,30] rearrangement of fulvalene diruthenium derivatives,[20,31,32] dihydroazulene - vinylheptafulvene photochromes, norbornadiene - quadricyclane, and others.[33,34] Some of these systems are illustrated in Figure 2.2.

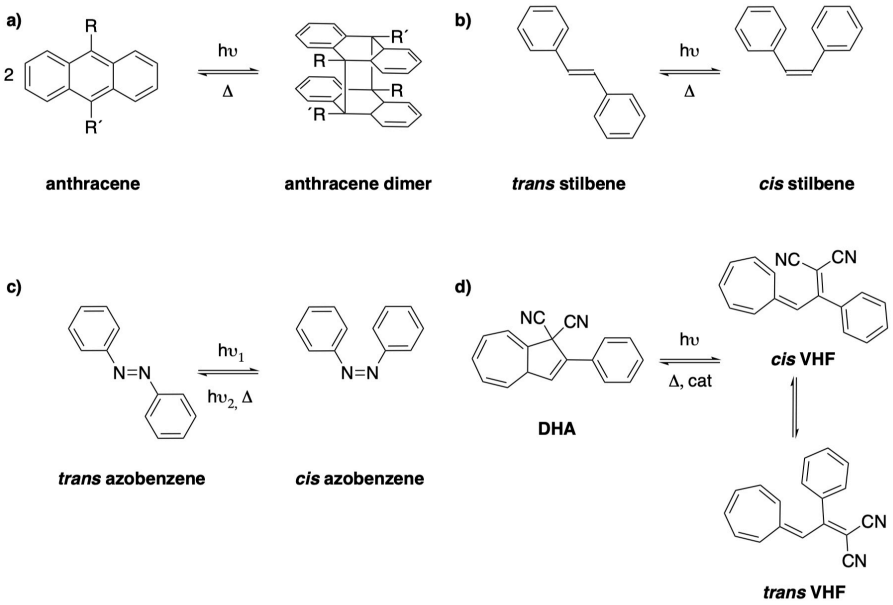


**Figure 2.2:** a) dimerisation of anthracene; b) *trans*/*cis* isomerization of stilbene; c) *trans*/*cis* isomerization of azobenzene; d) ring opening and closing of dihydroazulene-vinylheptafulvene.

Anthracenes undergo photo induced dimerisation, via [4+4] cycloaddition (see Figure 2.2a), and have been considered in the past as MOST candidates.[27,35] Anthracene absorbs strongly around 400 nm, while the dimer absorbs below 300 nm and can store about 65 kJ mol$^{-1}$. Introducing electron withdrawing (EWG) groups increases the energy storage density up to 84 kJ mol$^{-1}$.[27] The photodimerisation quantum yield has been measured up to 30% but it is, reasonably, concentration dependent. Interestingly, covalently linking two anthracene moieties made the photoisomerization concentration independent (with measured quantum yield up to 36%) and pushed the absorption onset up to about 500 nm. While linking the two anthracenes in a ring was expected to increase their energy storage, this decreases respect to other systems (measured energy storage up to 36 kJ mol$^{-1}$).[27]

The double bond of stilbene derivatives isomerise from *trans* to *cis* (as shown in Figure 2.2) when irradiated with light between 300 and 700 nm, making it an interesting candidate for MOST applications.[28] A significant drawback is although the very small energy storage density of the *cis* isomer (only 5 kJ mol$^{-1}$). It is very interesting to see how the energy storage of these systems was significantly improved by increasing the energy difference between the *cis* and *trans* isomers. Up to 104 kJ mol$^{-1}$ were achieved by stabilising the *trans* isomer with extended conjugated systems and at the same time introducing bulky groups that induce steric hindrance and destabilise the *cis* isomer.[36,37]

Azobenzene derivatives have been thoroughly investigated also as MOST materials, with interesting results which were recently summarised in a review.[38] Unsubstituted azobenzene undergo *trans* to *cis* isomerization when absorbing UV light (365 nm), with 49% quantum yield. The high energy cis isomer can store 49 kJ mol$^{-1}$, and it has a half-life of 4.2 days.[25,38] These parameters are not optimal for energy storage purposes, moreover the overlap between the *trans* and *cis* spectra, usually leads to the formation of a photostationary state. Azobenzenes have been widely investigated as functional materials with advanced features, such as sensors,[39] actuators,[40] optical data storage.[41] The first azobenzene derivatives that had been investigated for energy storage purposes did not achieve high performances, mainly due to the low energy storage density and poor photoconversion efficiency.[42] The theoretical work of Grossman *et al.* attracted new attention on azobenzenes for energy storage applications. He showed how packing azobenzenes on carbon nanotubes (CNT) would significantly increase the energy storage time and also the energy difference between the two isomers, therefore increasing the energy storage density of the material.[21] Preparation of densely packed azobenzenes anchored on CNT have

not been trivial. The materials that were eventually made and characterised reached 120 kJ mol$^{-1}$ in energy storage density, which was an increase with respect to the pristine systems, but still below the calculated values.[43,44] Graphene templated azobenzenes have been also fabricated and tested for MOST applications. Some of these materials reached energy storage densities of 572 kJ mol$^{-1}$ (up to almost 500 J g$^{-1}$), and half life of the charged material up to 5400 h.[38] Azobenzenes have also been attached to polymers, to achieve solid MOST materials;[45,46] these polymer films are very promising promising, buy had serious drawbacks which still need to be addressed, for example the photoisomerization had to be performed in the liquid phase, which implies that they are not fully operational in the solid polymer. Azobenzenes have been also combined with solid-liquid phase change materials (PCM) to improve their performances, which is an interesting and promising concept.[47] Heat is absorbed by the PCM, and UV light induced photoisomerization to the *cis* isomer increases the energy barrier to the recrystallisation, therefore increasing the storage time. Visible light can then be used to convert the azobenzenes back to *trans*, lower the barrier and allow the exothermic phase change.

Dihydroazulene–vinylheptafulvene (DHA-VHF) is a relatively recent photoswitch which has attracted a lot of attention as MOST candidate. DHA undergoes ring opening after irradiation with visible light. Systematic study of synthetic approaches and properties-relationship of DHA-VHF derivatives, supported by theoretical investigations and device testing were done. These allowed in depth understanding of DHA-VHF derivatives and significant advance toward their application as MOST. Some of the achievements are, for example, increased energy storage density, VHF life-time, and development of catalysts to efficiently trigger the thermal back reaction.[48–54]

## 2.3 Norbornadienes for MOST Applications

Norbornadiene (NBD) is an organic compound which undergoes a photo induced $[2+2]$ cycloaddition when exposed to UV light (Figure 2.3). The product is the highly strained and unsaturated quadricyclane (QC). The NBD-QC couple was first investigated in the early ´60s,[55,56] and it has been extensively studied in the past as candidate for MOST applications. The literature on this topic is fairly rich, and it has been the subject of several reviews and book chapters.[22,24,25,57–61]

NBD-QC have very high energy storage density (89 kJ mol$^{-1}$, corresponding to about 1 MJ kg$^{-1}$),[62] and high activation barrier for the back conversion

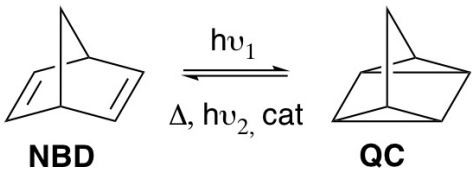


**Figure 2.3:** Photoisomerization and back conversion of Norbornadiene (NBD) and Quadricyclane (QC).

(which leads to a very long half-life of QC, measured as 14 h at 140 °C)[55]. Norbornadiene is commercially available (it costs about 200 euro for 250 mL from Sigma-Aldrich), and both NBD and QC are liquid at room temperature, which allows potential applications in closed flow systems without the need for a solvent. The main drawbacks of the NBD-QC system for MOST applications are the absorption onset ($A_{onset}$), which falls below 300 nm (outside the solar spectral window), and the low quantum yield of photoisomerization $\phi$ ($\sim$5%).[63]Tackling these main issues, without compromising the other properties, is fundamental in order to achieve a functional NBD-QC based MOST system.

Donor and acceptor groups on the two double bonds, or a donor and acceptor group on one double bond have been introduced in the past to red-shift the absorption of NBDs. Two research groups have been particularly prolific, Dubonosov *et al.*[61,64–66] and Yoshida *et al.*,[23,63,67,68] and a great deal of norbornadiene derivatives have been synthesised and their properties characterised, which have also been summarised in the aforementioned reviews.[24,25,57,59,60] Typical norbornadienes synthesis have traditionally relied upon Diels-Alder cycloaddition reactions of modified cyclopentadienes with acetylene derivatives.[23,57,60,69] Conjugating donor and acceptor groups to the olefins of the NBDs revealed to be an efficient strategy, and many of these derivatives exhibit $A_{onset}$ up to 400-500 nm, often with high $\phi$.[23,57,60] Some compounds with $A_{onset}$ of 580 nm[70] or even as high as 700 nm[71] have been made, but they tend to have dramatic drawbacks like degradation, very low activation energy for the back conversion or low $\phi$. To improve $\phi$, the use of triplet sensitisers (as acetophenone) have been explored, often successfully.[55–57,59,72,73] Catalysts for triggering the back isomerization of QC have been developed and tested,[67,74] and some demonstration devices have been designed and tested too.[75] Interestingly, norbornadiene derivatives have also been mixed in polymeric solid films, maintaining the overall properties, and achieving outstanding stability over thousands cycles.[63] Norbornadiene moieties have been also incorporated into polymers.[70,76–78] Research in this field seemed to come to a halt after a quite optimistic review in 2002.[60] More recent work from

Yoo, Tam and coworkers,[79,80] introduced a new synthetic protocol for synthesising substituted norbornadienes, based on the Suzuki-Miyamura coupling reaction. The possibility of accessing new classes of norbornadiene derivatives, together with more advanced computational methods, sparked a renewed interest in this class of compounds. This resulted in the synthesis and characterisation of new derivatives with donor-acceptor groups and low molecular weight.[81,82] These studies were complemented by theoretical insights.[83,84] It is about at that time that the work presented in this thesis started, and in the following section some of the challenges that needed to be addressed will be discussed.

## 2.4 Open Challenges

A challenge that has not been overcome yet is to design, synthesise and characterise a compound with all the aforementioned properties fully optimised. An ideal compound with all the parameters optimised does not seem to exist yet. This is not an easy challenge, since the ideal properties depend on the chosen application. Moreover, it is fundamental to keep in mind the potential, properties and limitations of a MOST systems, which have been previously discussed.[26]

In order to optimise NBD-QC systems for MOST applications, it is necessary to develop strategies to selectively engineer the different properties. The introduction of electron withdrawing and electron donating groups allowed to significantly red-shift the absorption onset of NBD and serendipitously make promising candidates. But at the time this project was started there were almost no available strategies to selectively and efficiently control the energy storage density, the photoisomerization quantum yield, or the activation energy for the back conversion. Moreover, both quantum yield and QC lifetime seemed to often decrease when the absorption spectrum was red-shifted. The NBD-QC system is an extremely versatile system, and its properties can change within a very wide range of values, depending on the chemical modifications.

An important tool to design new optimised norbornadienes is the use of theoretical calculations. In the last years some works have been published where theoretical modelling have been used to predict and screen new norbornadienes.[83] This is an important challenge, and while some parameters can be predicted very accurately, others are harder to simulate. One example is the activation energy for the back conversion $\triangle G^{\ddagger}$, which is a key parameter, but is not always well predicted with the available models.

There are still a lot of open challenges and the field needs to be further ex-

plored to its full potential. The work presented in this thesis will try to address some of these challenges.

The main scientific questions that motivated the work discussed in the next chapters are the following:

- Is it possible to selectively engineer the activation energy for the thermal back isomerization in NBD-QC based MOST, without compromising the other properties, especially the energy storage density?
- What are the possible applications of a MOST technology? Can laboratory-scale test devices be of help in identifying potential applications at a research level?
- Is it possible, and convenient, to obtain functional neat liquid norbornadiene based MOST materials?
- What are the other potential applications of NBD-QC photoswitches?

# Chapter 3

# Design, Synthesis and Characterisation of New Norbornadienes for MOST Applications

*In this chapter norbornadienes syntheses, and their key photochemical and thermodynamic properties will be presented one by one. Work mainly published in Papers I and II is discussed and put into context.*

## 3.1 Synthesis of New Norbornadienes

*In this section the synthesis of some norbornadiene derivatives (published in appended Paper I) is presented. The chosen synthetic strategy is discussed and compare with other recent approaches.*

Chemical modifications on the NBD backbone is of great interest in order to investigate structure properties relationships. An in depth knowledge of these relationships allows selectively engineering the individual properties of NBDs to match desired properties for MOST applications. The syntheses were done as for now mostly in small scales for research purpose, but the synthetic methods will have a big impact on the development of the final product. It is therefore important to identify synthetic methods that allow exploration of a wide range of compounds on a research level, but also highlight cheap and available starting

materials, and simple and scalable syntheses.

NBD synthesis through Diels-Alder reaction has been reported already in 1956.[85] Since then, a great deal of NBD derivatives have been made for different purposes, included as intermediates for the synthesis of bioactive compounds, memory devices, MOST applications, or more.[69] A comprehensive review on the synthesis of modified NBDs was published in 2013 by Tam *et al.*[69] A large number of NBD derivatives for MOST applications have been synthesised, and are best summarised in previous reviews and book chapters.[23–25,57,59,60]

Synthesis of substitute norbornadienes relies nowadays mainly on two different approaches, as seen in Figure 3.1: Diels-Alder cycloaddition reaction between modified cyclopentadienes and acetylenes, or post modifications on the commercially available norbornadiene. In the recent years, advances in the latter approach involved introduction of halogens on the double bonds of NBD, and subsequent coupling reactions (such as Suzuki or Sonogashira coupling) to easily introduce a wide range of groups in these positions.[79,81,82,86]

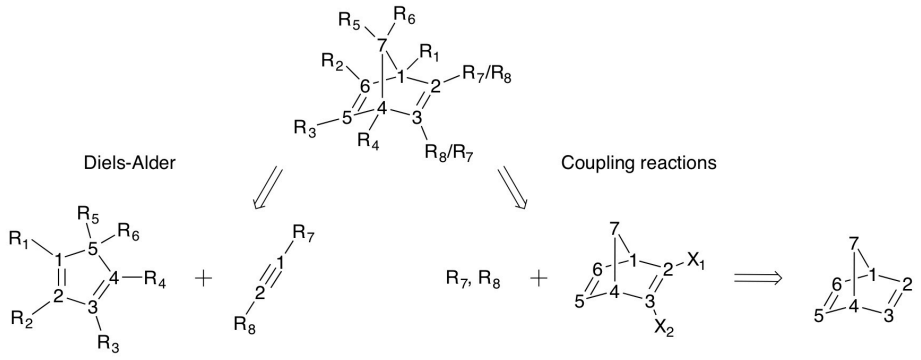


**Figure 3.1:** Retrosynthesis scheme showing commonly used approaches for the synthesis of a wide range of NBD derivatives.

Diels Alder reactions have been used for many years to make NBD derivatives, and are an efficient and versatile approach; this was chosen to make a serie of NBD derivatives (published in appended Paper I). Limitations are induced by the mechanism of the reaction. It is possible to introduce substituents in any of the position on the cyclopentadiene or acetylene, but especially the electronic properties of the substituents have to be considered carefully to not interfere with the mechanism of the cycloaddition reaction. Cyclopentadiene is an excellent diene for D-A reactions; it is electron rich (which is favourable in normal electron-demand D-A) and already locked in the optimal conformation to react in the D-A. Substituents on the cyclopentadienes should not alter its electronic properties significantly: electron withdrawing substituents would slow down the D-A reaction, and electron donating substituents risk to make it so reactive that

it will immediately dimerise.[87] Moreover, the hydrogens of cyclopentadiene are subjected to facile thermal sigmatropic rearrangements, producing a mixture of structural isomers after a short time at room temperature.

Acetylene is not a good dienophile, but electron withdrawing substituents can improve its reactivity in D-A with dienes.[88] In the specific case of the NBDs serie published in Paper I, an electron withdrawing and an electron donating group were wanted on at least one of the norbornadiene double bond, which could be introduced on the acetylene derivative. These requirements are limiting the choices in terms of acetylene derivatives when synthesising NBDs for MOST applications using D-A reactions.

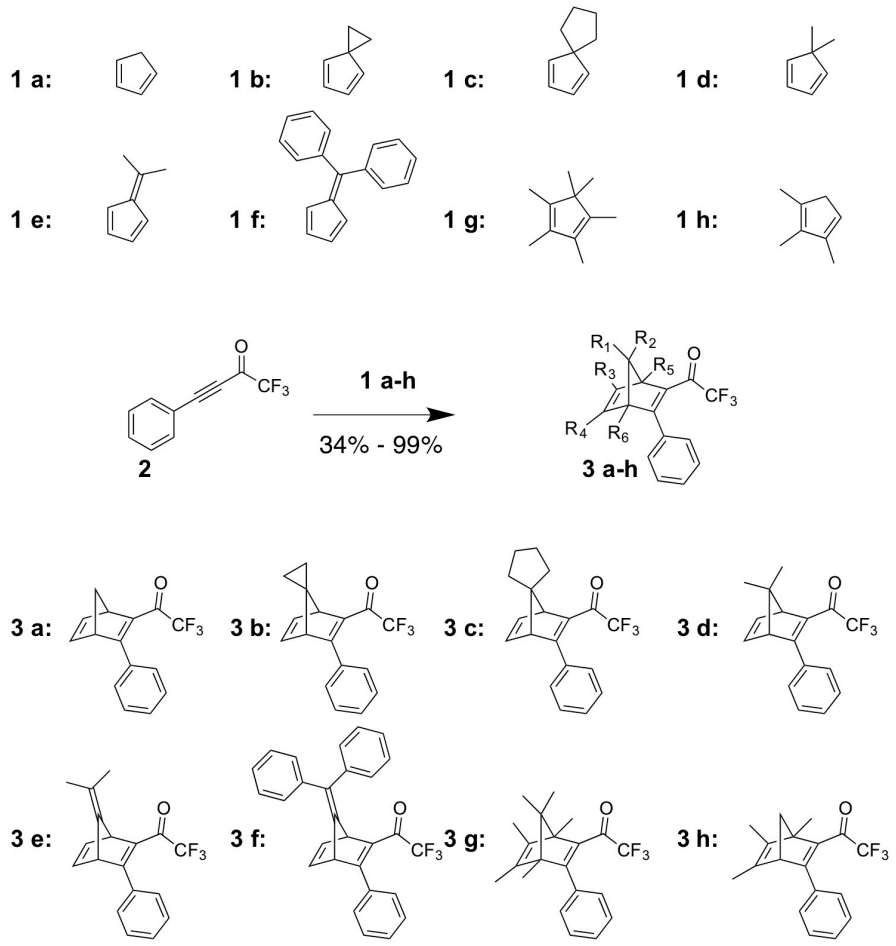


**Figure 3.2:** Performed synthesis of NBD derivatives, based on Diels-Alder cycloaddition reactions of modified cyclopentadienes and acetylene.

In Figure 3.2 are shown some of the synthesized compounds. Small alkyl groups were added to the cyclopentadienes, and when possible two alkyl groups were introduced on C5, to prevent sigmatropic shifts. Some of the used cyclopentadienes were commercially available (**1a**, **1e**, **1f**, **1g**), the others were all known compounds,[89–93] and some were synthesised in collaboration with Jonas

Udmark from Copenhagen University (**1a**-**c**, **3b**). Acetylene **2** in Figure 3.2 was chosen after careful literature research as a promising acetylene for the purpose of this project. It is a known compound that have been previously reported in D-A reactions (also with cyclopentadienes **1a** and **1b**).[94] This acetylene is simple to synthesise, as it is obtained in one step from the commercially available ethyl ester.[95] It reacts extremely well in the D-A, and it affords norbornadienes with a polarised and delocalised double bond. Norbornadienes **3a**-**h** in Figure 3.2 were synthesised by reacting cyclopentadienes **1a**-**h** with acetylene **2**. The obtained norbornadienes were mostly in the form of oil at room temperature (compounds **3a**-**d**). The D-A reactions were quite insensitive to the used solvents, and proceeded in many cases also under solvent free conditions (which would be a favourable choice when scaling up the reactions). The use of a microwave reactor resulted in significant reduction of the reaction time from days to hours. The yields are from acceptable to very good for the different compounds (from 34% to almost quantitative) and could be possibly improved in some cases by reducing the reaction time. In summary, the chosen acetylene and overall synthetic approach is versatile, efficient, simple and potentially scalable. A similar synthetic approach, based on D-A of modified cyclopentadienes and acetylene derivatives, was used by K. Jorner in the appended paper II.[96] It afforded a series of NBDs derivatives with donor acceptor groups on the two double bonds and different alkyl groups on the C7 position (see Figure 3.3 a). Functionalisation of di-halogenated NBD derivatives through Suzuki or Sonogashira coupling with appropriate substituents was instead used in our group by Gray *et al.*[81] and Quant *et al.*,[82] to afford a range of 2,3 substituted NBDs (see Figure 3.3 b). This approach was first used by Tam *et al.*,[79] and it has the advantage to allow easy preparation of derivatives that would be difficult to obtain through the D-A approach. Moreover it is convenient to use the same precursor (di-halogenated NBD **11** in Figure 3.3 b) for a wide range of reactions. However, in the perspective of future scale up, the D-A approach has many advantages. It allows solvent free conditions, it involves fewer steps and gives higher yields, and it does not require the use of expensive catalysts like in the coupling reactions.

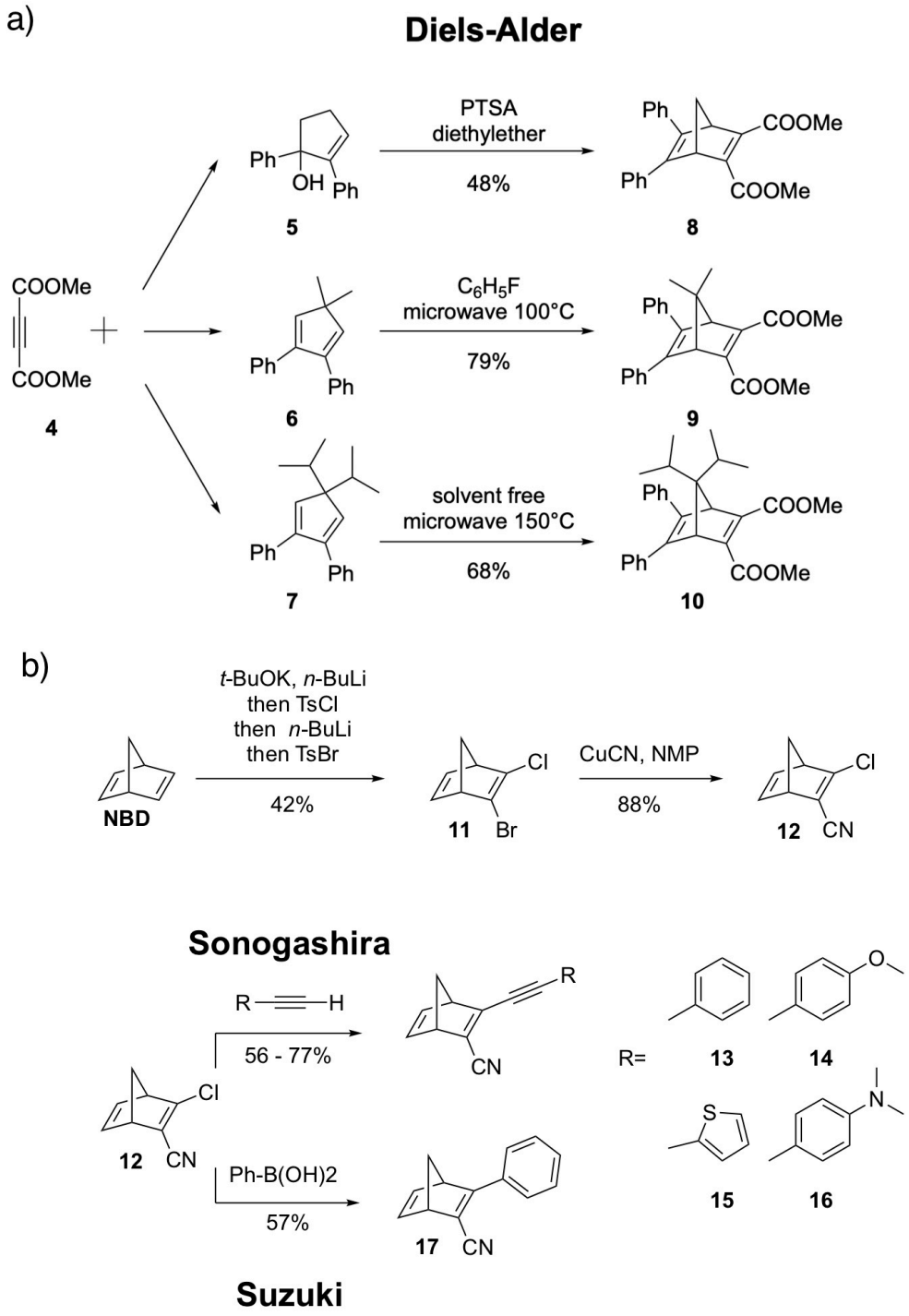


**Figure 3.3:** Recent alternative synthetic approaches to NBD derivatives for MOST. a) Synthesis of substituted NBDs based on Diels-Alder reactions of modified cyclopentadienes and acetylene, done by K. Jorner in appended paper II.[96] b) Synthesis of NBDs done by M. Quant, based on coupling reactions (Sonogashira and Suzuki) of halogenated NBD **11**.[82]

## 3.2 Tuning the Absorption Spectra of Norbornadienes for MOST Applications

*In this section the spectral properties of norbornadienes are presented, and discussed from the perspective of MOST applications. The spectral properties of the synthesized compounds (published in appended Paper I) are presented and compared with others.*

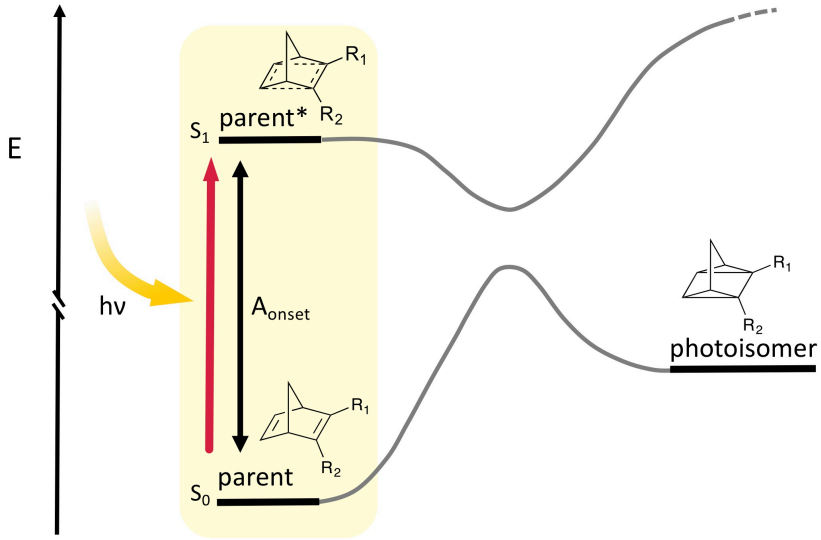


**Figure 3.4:** Energy scheme of a NBD-QC system, showing absorption of light by the parent system, and the energy corresponding to the absorption onset ($A_{onset}$) of norbornadiene. The absorption process is indicated as a red arrow.

Appropriate optical properties are of fundamental importance in order to make efficient MOST materials. The absorption spectrum of the MOST should overlap as much as possible with the solar spectrum. It is also important for the high energy isomer to not absorb the sun photons, in order to not compete for it with the parent isomer. For this reason the intrinsic properties of the NBD-QC system are favourable, since the photoisomerization involves the breaking of double bonds and the formation of single bonds, and the QC spectrum is therefore blue-shifted. It is also in general undesirable to have light induced photoisomerization of the high energy isomer back to the parent isomer. This can be avoided or minimised by choosing a system where this photoisomerization is not allowed or not efficient, or by having a high energy isomer with low absorption above 300 nm.

In Figure 3.4 it is shown the energy scheme of a generic NBD-QC system. As presented in Chapter 2, the energy difference between the parent isomer and its excited state $S_1$ correlates to the absorption onset ($A_{onset}$) of the system. It

is therefore beneficial to decrease the $S_0 - S_1$ gap in order to absorb as many as possible of the solar photons. As we have seen previously, NBD spectral properties have been tuned by introducing a wide range of substituents.[57,59,60] Successful approaches involved introducing donor and acceptor substituents, on the two double bonds and interacting through space, or conjugated through one of the double bonds. The latter approach has been recently preferred because it allows to red-shift the NBD absorption significantly, avoiding sensitisers induced side reactions, while keeping the molecular weight low (and therefore the energy storage density high).

**Table 3.1:** Spectral properties of synthesised norbornadienes **3a-h**, and published norbornadienes **8**,[96] **16**,[81] **18**[82] for comparison. UV-Vis spectra of **3a-h** were measured in toluene. Molecular weights are reported too. $A_{onset}$ is defined as the wavelength where log($\varepsilon$)=2.

| Compound | $\varepsilon_{max}$ $(M^{-1}cm^{-1})$ | $A_{max}$ $(nm)$ | $A_{onset}$ $(nm)$ | $MW$ $(g\,mol^{-1})$ |
|---|---|---|---|---|
| **NBD** | - | - | <300 | 92 |
| **NBD 3a** | $5.2\times10^3$ | 323 | 426 | 264 |
| **NBD 3b** | $5.5\times10^3$ | 341 | 431 | 290 |
| **NBD 3c** | $6.1\times10^3$ | 326 | 436 | 318 |
| **NBD 3d** | $5.7\times10^3$ | 323 | 439 | 292 |
| **NBD 3e** | $4.9\times10^3$ - $3.4\times10^3$ | 305 - 364 | 437 | 304 |
| **NBD 3f** | $6.0\times10^3$ - $3.0\times10^3$ | 309 - 363 | 445 | 429 |
| **NBD 3g** | $1.4\times10^3$ | 346 | 426 | 348 |
| **NBD 3h** | $2.5\times10^3$ | 350 | 439 | 306 |
| **NBD 8** | $2.5\times10^3$ | 341 | 391 | 360 |
| **NBD 16** | $30\times10^3$ | 398 | 456 | 260 |
| **NBD 18** | $8.0\times10^3$ | 308 | 389 | 244 |

Due to the presence of the electron donating (EDG) and electron withdrawing (EWG) groups on the double bond of the synthesised NBDs **3a**-**h**, their absorption spectra is red-shifted into the visible range, with $A_{onset}$ up to about 450 nm. Parameters from the recorded absorption spectra are reported in Table 3.1. Optimised $A_{onset}$ for seasonal heat storage has been theoretically defined as about 600 nm, and there have been previously reported compounds which reached up to 700 nm, but with drastically low $\phi$.[71] Very few compounds with $A_{onset}$ up to or above 400 nm have overall good properties for MOST;[97] they often exhibit very low $t_{1/2}$,[97] $\phi$,[61,71] or degradation issues.[97,98] In the synthesized series, and especially in the case of **3a**, satisfying spectral features are obtained with very few synthetic steps, and maintaining good overall properties (as MW, half-life of QC and energy storage density, which will be discussed in later sections). The compounds synthesised by K. Jorner in appended Paper II have also quite red shifted spectra ($A_{onset}$ = 391 nm), but the molecular weight is higher (**8** has a

MW of 360 g mol$^{-1}$, compared to **3a** which has 264 g mol$^{-1}$), and therefore their energy storage density is decreased also for this reason.

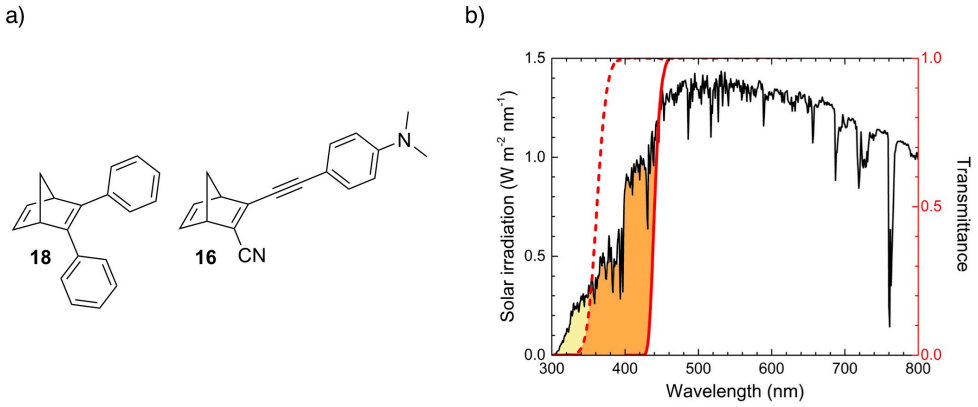


**Figure 3.5:** a) Previously made norbornadienes **18** and **16**.[81,82] b) Solar irradiation spectrum and transmittance of a solution of **18** and **16** in toluene. **18** absorbs the yellow portion of the spectrum (3.8%), while **16** absorbs also the orange part (12%). Image used with permission from RSC.

Norbornadiene **18** in Figure 3.5 has been previously synthesised and characterised in our group, and has $A_{onset}$ = 389 nm,[81], while **16** has $A_{onset}$ = 456 nm. If we look at the solar spectrum in Figure 3.5, these 100 nm are of extreme importance, since in this range there is a significant increase of solar irradiation. Assuming that all photons below the $A_{onset}$ are absorbed, NBD **18** absorbs 3.8% of the solar spectrum, while **16** absorbs up to 12%; this will significantly affect the performance of these compounds the device test, as it will be discussed in Chapter 4.

## 3.3 Quantum Yield of Photoisomerization

*In this section the quantum yield of NBD to QC photoisomerization is presented. Its importance for MOST applications and ways to improve it are discussed. The values measured for the series of synthesized compounds (appended Paper I) are presented and compared with other published results.*

Once a NBD molecule has absorbed a photon, it will be in an excited state, and after fast vibrational relaxation to $S_1$ different processes can occur. After relaxation to a local minimum, it can relax to the original parent molecule, or photoisomerise to QC through a conical intersection. Photoisomerization is usualy accompanied by a typical decrease of the absorption band of the NBD, since the QC spectrum is blue-shifted.The photoisomerization quantum yield $\phi$ expresses

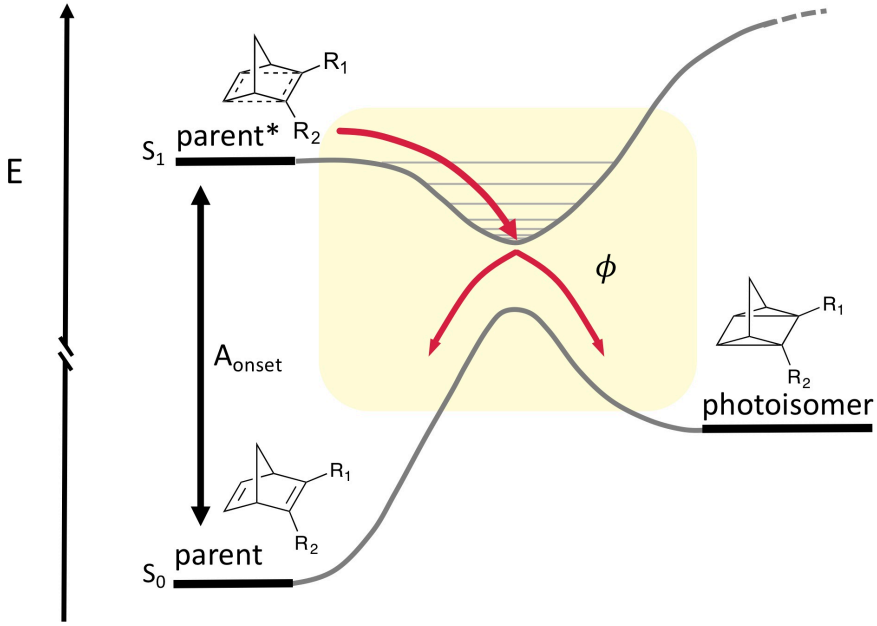


**Figure 3.6:** Energy scheme of a NBD-QC system, showing some of the possible relaxation pathways of NBD* from the excited state $S_1$ (in red arrows). The different pathways can lead to the original NBD, or to the photoisomer QC, where the photoisomerization quantum yield $\phi$ express the probability of the latter to happen.

the probability of the photoisomerization event to happen. Radiative decay would be a competing process, but it very rarely occurs in NBD systems.[99]

For MOST applications it is important for the photoisomerization quantum yield $\phi$ to be as near as possible as 100%, but often this is not the case. Of all the studied compounds in the past literature, values from very low (as 5% for NBD)[63] to 100%[23] have been measured. Some trends have been observed before,[65] but rational strategies to increase $\phi$ by molecular modifications did not really exist when the work presented in this thesis was started. In some cases (as for unsubstituted NBD) the preferred photoisomerization mechanism is thought to involve intersystem crossing (ISC) to a triplet state and then relaxation to QC, and it is therefore favoured in the presence of triplet sensitisers.[57,60] In other cases, the preferred mechanism is on the $S_1$ surface, and triplet sensitisers do not facilitate the photoisomerization.[100]

Photoisomerization quantum yields to the respective QC isomers have been measured for all the synthesised compounds **3a**-**h** (appended Paper I). This was done by using a chemical actinometer to measure the irradiation photon flux, and by correlating the observed photoisomerization in optically dense toluene solutions after defined irradiation times; the method is described in more detail in the Methods Chapter. The measured values can be found in Table 3.2. Norbor-

**Table 3.2:** Measured quantum yield of NBD to QC photoisomerization ($\phi$) in toluene solutions of compounds **3a**-**h** (at 365 nm). The published values of **NBD**, **8**-**10**,[96] **16**[82] and **18**[81] are reported for comparison.

| Compound | $\phi$ (%) |
|---|---|
| **NBD** | 0.05 |
| **3a** | 53 |
| **3b** | 45 |
| **3c** | 51 |
| **3d** | 55 |
| **3e** | 45 |
| **3f** | 34 |
| **8** | 73 |
| **9** | 86 |
| **10** | 88 |
| **16** | 28 |
| **18** | 60 |

nadienes **3a**-**d**, have all $\phi$ of about 50 %, which is a good value for energy storage applications. Interestingly, NBDs **3g**-**h** irreparably degraded upon irradiation with light, which could be correlated to the vicinity of the methyl on the bridgehead and carbonyl group on the double bond. This was surprising since other NBDs bearing methyl groups on the same bridgehead were not reported to degrade.[23] The exact causes and mechanism of the degradation were not identified, but this molecular design was discarded for obvious reason. While these observations did not find a space in Paper I, it is still important to report them.

In appended Paper II, theoretical calculations done by K. Jorner showed how introducing bulky groups on the C7 (bridge) position correlates with increased quantum yield (see values for **8**-**10** in table 3.2), increased half-time of QCs and decreased energy storage density. With insights from DFT calculations, it became clear how the $\phi$ trend is due to the destabilisation of NBDs induced by the steric pressure from the bulky groups. Destabilisation of the NBDs induces changes to the energy landscapes, so that the energy barrier on $S_0$is moved toward the NBD isomer. Because of this, the position of the conical intersection end up being more on the QC side of the energy barrier, and therefore the photoisomerization quantum yield is increased. The drawback is that destabilisation of NBD is accompanied by a decrease in energy storage density. This result is of great interest, since it correlates stabilisation effects on NBDs to the photoisomerization properties, and it is a useful tool for engineering the photoisomerization quantum yield in future designs.

## 3.4 Energy Storage Density of MOST

*In this section the energy storage density of MOST materials is presented. The measured values are reported, and ways to improve this parameter are discussed.*

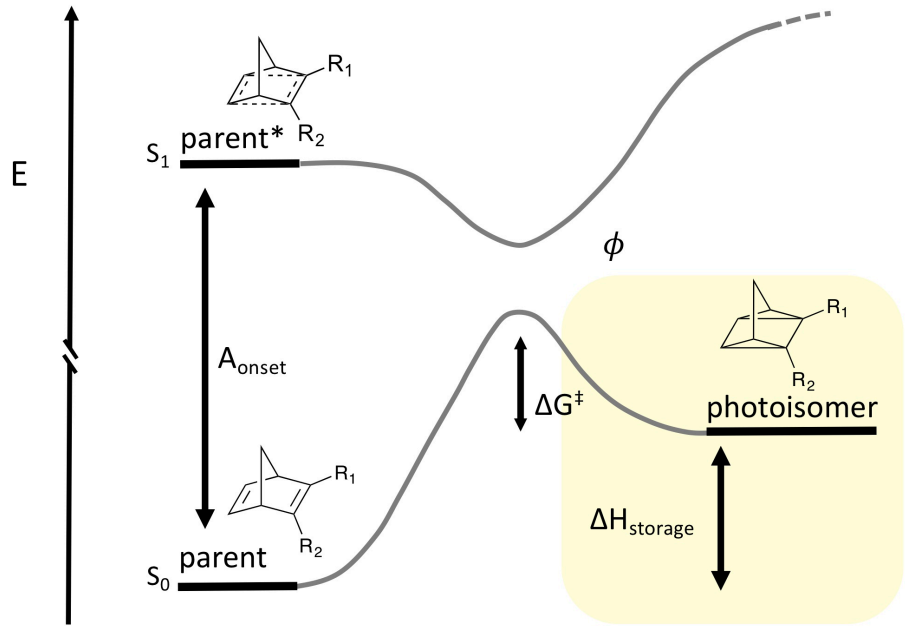


**Figure 3.7:** Energy scheme of a NBD-QC system, showing the energy difference between QC and NBD, which corresponds to the stored energy.

The energy difference between QC and NBD isomer corresponds to the energy that is, in fact, eventually stored by the MOST material. This energy rise mainly, in this case, from the high strain in the QC bonds. Unsubstituted quadricyclane can stores a large amount of energy (about 1 MJ $mol^{-1}$)[62], which could potentially translate to a $\Delta$T of 600 °C. Water, in comparison, can store 209 J/g,[101] and modern Li-ion batteries can reach energy densities up to 875 J/g.[102] Unfortunately, unsubstituted norbornadiene does not absorb in the visible range; it has been discussed previously how substituted norbornadienes could theoretically reach about 480 J/g.[26] Considering a $C_P$ equal to the one measured for NBD, this value could translate to a temperature increase of 289 °C, which would be useful for a range of applications where medium/ low heat is needed.[18]

Nowadays the released heat is in most cases measured using differential scanning calorimetry (DSC), which was also done on all the compounds synthesised in the MOST team. The energy storage densities of the QC isomers of **3a**-**d**, **8**-**10**, **16**, were measured, and are reported in Table 3.3. The presented

**Table 3.3:** Measured energy storage enthalpies of QCs **3a**-**d**, **8**-**10**, **16**. Literature values of QC,[62] and calculated values are reported for comparison.

| Compound | $\triangle H_{storage}$ $(kJ\ mol^{-1})$ calculated | $\triangle H_{storage}(kJ\ mol^{-1})$ measured | $\triangle H_{storage}$ $(J\ g^{-1})$ measured | $\triangle T$ (°C) predicted |
|---|---|---|---|---|
| **QC** | 93 | 92 | 1000 | 602 |
| **QC 3a** | 100 | 152 | 577 | 349 |
| **QC 3b** | 98.4 | 103 | 354 | 213 |
| **QC 3c** | 92.1 | 48 | 152 | 92 |
| **QC 3d** | 84.2 | 49 | 167 | 100 |
| **QC 3e** | 88.4 | - | - | - |
| **QC 3f** | 84.5 | - | - | - |
| **QC 8** | 82.4 | 85 | 236 | 142 |
| **QC 9** | 69.9 | 68 | 176 | 106 |
| **QC 10** | 58.2 | 46 | 104 | 62 |
| **QC 16** | 124 | 103 | 396 | 238 |
| **QC 18** | 111 | 86.5 | 354 | 213 |

results have been published in appended Papers I, II and III respectively. These are compared with the published values of NBD, **18**,[84] and to the calculated values (calculations done by K. Jorner,[96] Z. Wang,[103] or Erhart *et al.*[82,84]).

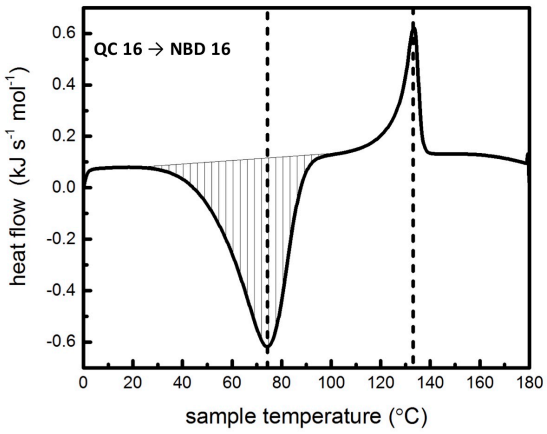


**Figure 3.8:** The measured DSC thermogram for compound **16**.[82]

Energy densities were measured by producing a small amount of the relative QC isomer by irradiation, and inserting a neat sample (accurately weighed and sealed in an aluminium pan) in a DSC machine. The sample was then subjected to multiple cycles of heating and cooling. Heat was released during the first cycle of heating, and not during the second one. The area of the measured exothermic peak (see example in Figure 3.8) was then normalised by the weight of QC, to give the storage energy density. In most cases the measurements gave accurate and reliable values. Moreover, back isomerization of QC while preparing the

samples was accounted by measuring an NMR on a sample at the same time of the DSC experiment, and correcting the amount of QC accordingly. For few molecules some difficulties arose, and different solutions were found in order to obtain some indicative values; in these cases the measured values were always reported together with the calculated values. In some cases the back conversion was so fast (**3a**-**d**) that the only way to measure some heat release was to irradiate the DSC samples for a long time until discolouration was observed by eye, and then immediately inserting the samples in the DSC machine. It is understandable that back conversion of QC made these values an underestimation. The measured energy density of **3a** is strangely higher than the calculated value, which was suggested could be due to degradation. In some cases it has not been possible to measure any value, because of significant degradations (**3e**-**f**) or because potential concurring phase changes (as for example for **13**-**15**, published by Quant *et al.*).[82] NBD has, as previously mentioned, a very high energy storage density, but overall poor properties as MOST. Compound **3a** stands out as very promising, with good energy storage density, and overall properties (as easy synthesis, red-shifted absorption, high $\phi$, long $t_{1/2}$ as will be discussed later). Looking at the energy diagram in Figure 3.7, and learning from past examples, it is easy to see how both a stabilisation of NBD, or a destabilisation of QC would lead to an increase in energy storage density. The first case would imply also blue-shifting of the absorption spectrum, while the latter would most likely affect negatively the half-life of QC. Chemical modifications have to be done with groups as small as possible, to keep the MW as low as possible and not decrease the energy storage density. The overall properties of the system have to be also satisfying, which is usually the biggest challenge (as in the example of unsubstituted NBD). It is important to note that the systems should eventually work in neat or highly concentrated form, since diluting or mixing would obviously decrease the energy storage density. While the measured energy storage densities are usually satisfying if evaluated for medium/low heat applications, in most of the studied cases the properties (as $A_{onset}$,$\phi$, or $t_{1/2}$) were often below the desired targets. Slightly compromising the energy storage density in favour of other key properties could be a viable strategy toward overall better performing systems in future designs.

## 3.5 Activation Energy for the Thermal Isomerization of Quadricyclane to Norbornadiene

*In this section the kinetic stability of quadricyclanes is examined. The measured values (Paper I and II) are presented, and different strategies to efficiently increase the energy storage time are discussed.*

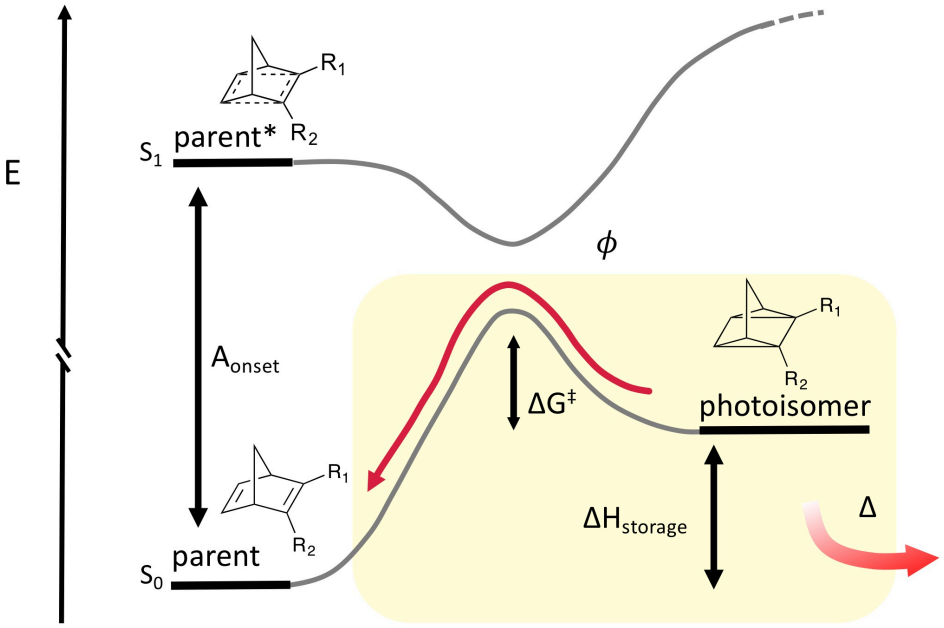


**Figure 3.9:** Energy scheme of a NBD-QC system, showing the energy barrier $\triangle G^{\ddagger}$ for the thermal isomerization of QC to NBD. The isomerization process is indicated with a thin red arrow. The heat release which accompanies the isomerization is also indicated with a wide red arrow.

Quadricyclane is a high energy molecule which is kinetically stable also for long times, but it does eventually thermally back isomerise to norbornadiene. The kinetic stability of quadricyclanes is a key parameter in order to use them to store solar energy. While unsubstituted quadricyclane has an extremely long half-life ($t_{1/2}$ = 11 h at 150 °C),[104] chemical modifications, introduced mainly to optimise other parameters, often affect it negatively.[81,82] In the work by Börjesson *et al.* it is discussed how the energy barrier can be considered as a sort of "loss" of the energy absorbed from NBD, which is clear when looking at the energy scheme in Figure 3.9. In the same work it is calculated how a $\triangle G^{\ddagger}$ value of 120 kJ/mol allows a QC half-life of 1400 days, which is good for seasonal storage applications; for day to night storage applications it is enough with a $\triangle G^{\ddagger}$ of 110 kJ/mol.[26]

NBD derivatives with half-lives from years to minutes have been made,[59] therefore this property can be potentially tailored to best fit the desired applic-

ation. When this project was started there was really no method to selectively engineer the activation energy to the thermal isomerization of QC to NBD. In the previous literature some trend emerged, for example it seems that red-shifting the $A_{onset}$ is often accompanied by reduced $t_{1/2}$ of QC.[81] One way to increase $\triangle G^{\ddagger}$ could be by stabilisation of QC, but this would happen at the expenses of the energy storage density, which is usually undesirable.

**Table 3.4:** Measured kinetic parameters for the thermal back isomerization of QC isomers to NBDs **3a**-**d** and **8**-**10** in toluene solutions. Published values of QC,[104] **16**,[82] **18**,[81] **19**-**22**[105] are reported for comparison.

| Compound | $t_{1/2}$ @25℃ | $\triangle G^{\ddagger}$ @25℃ ($kJ\ mol^{-1}$) | $\triangle H^{\ddagger}$ ($kJ\ mol^{-1}$) | $\triangle S^{\ddagger}$ ($J\ mol^{-1}\ K^{-1}$) |
|---|---|---|---|---|
| **QC** | 83000 y | 145 | 154 | 31 |
| **QC 3a** | 72 h | 105 | 74.9 | -100 |
| **QC 3b** | 128 h | 106 | 85.6 | -69 |
| **QC 3c** | 48 h | 104 | 81.2 | -76 |
| **QC 3d** | 84 h | 105 | 80.3 | -83 |
| **QC 8** | 6.3 h | 99 | 89.5 | -31 |
| **QC 9** | 7.7 h | 99 | 89.7 | -32 |
| **QC 10** | 56 h | 104 | 90.7 | -45 |
| **QC 16** | 5 h | 98 | 92.5 | -19 |
| **QC 18** | 42 d | 112 | 109 | -9 |
| **QC 19** | 89.8 d | 113.3 | 116.3 | 10.2 |
| **QC 20** | 2680 d | 121.6 | 179.9 | 195.5 |
| **QC 21** | 78 d | 112.9 | 116.4 | 11.8 |
| **QC 22** | 2273 d | 121.3 | 134.4 | 44.1 |

Half-life of QCs were measured for the synthesised compounds **3a**-**f** (published in appended Paper I). Unfortunately, it was not possible to characterise the kinetics of **3e** and **3f** since they have a very long half-life, but also degraded during the process. The back isomerization of QC **3a**-**d** was characterised by following the isomerization at different temperatures and using the Eyring equation[106,107] to calculate half-lives, free energy, enthalpy and entropy of activation. The half-lives of these QCs was in general above 2 days, which is unusually high for compounds with such red-shifted absorption (for example **16** has $t_{1/2}$= 5 h,[82] as reported in Table 3.4).

After measuring the half-life of the QCs **8**-**10** (published in Paper II) it was observed how the $t_{1/2}$ of **10** was significantly higher than the other two (56 h, respect to 7.7 h and 6.3 h, values are in Table 3.4). Moreover, characterisation of the enthalpy and entropy of activation gave a significantly higher negative value of $\triangle S^{\ddagger}$ for **10**, while the $\triangle H^{\ddagger}$ were comparable (see Table 3.4). We formulated an hypothesis that the rotation of the isopropyl (iPr) groups is hindered in the NBD

isomer, while there is more space in the QC isomer therefore iPr can rotate more freely.

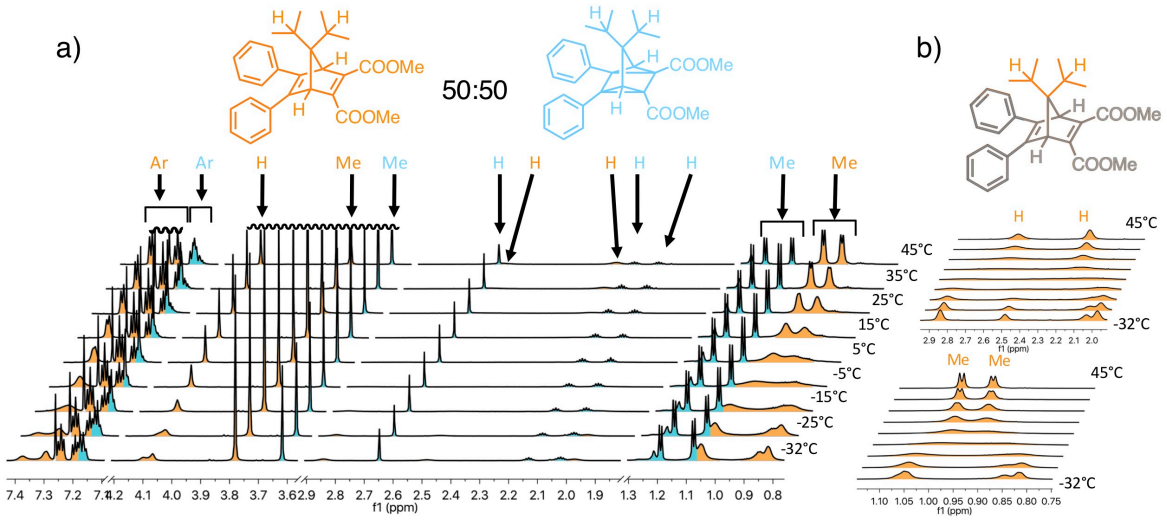


**Figure 3.10:** a) $^{1}$H NMR spectra of a 50:50 toluene solution of NBD and QC isomer of **10** measured at temperatures between -32 °C and 45 °C. Peaks from protons on NBD are filled in blue, the ones from QC are filled in orange. b) detail of the peaks from the iPr protons on QC **10** between -32 °C and 45 °C. Reproduced with permission of RSC.

$^{1}$H NMR peaks of the iPr were in fact broad in the NBD isomer, which can be due to hindered rotation, while they were sharp in the QC NMR. Variable temperature (VT) NMR spectra of a mixture of both NBD and QC of **10** were recorded and are shown in Figure 3.10. iPr protons of the QC are in slow conformational exchange with respect to the NMR timescale at low temperature (-32 °C), coalesce at about -5 °C, and are then in fast exchange at 45 °C (orange peaks in Figure 3.10). Instead, NBD iPr signals did not change over this range of temperature (blue peaks in Figure 3.10). These observations supported our hypothesis, confirming that the hindered rotation of iPr groups in the NBD isomer of **10** is the cause of the high negative activation entropy in the isomerization of QC to NBD, which makes the QC isomer having a longer half-life compare to **8** and **9**. These findings give a valuable insight on the thermal isomerization of QC, which can be used in future designs to selectively increase the half-life of QC without negatively affecting other properties.

Another recent work published by Jevric *et al.*[105] presents a similar but substantially different strategy to increase the activation energy of the back isomerization of QCs. A series of donor-acceptor NBDs were made by Jevric *et al.*, with cyano and aryl substituents. These have different substituents in *ortho*, *meta* or *para* position, and some of the studied compounds are shown in Figure 3.11. Characterisation of the kinetic, thermodynamic and photochemical properties re-

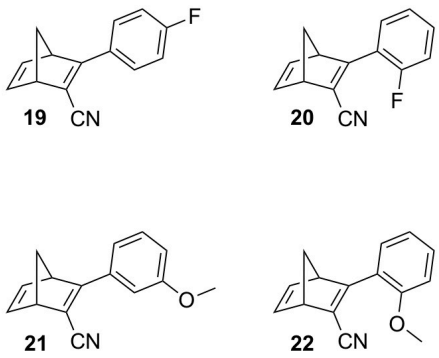


**Figure 3.11:** Recently made NBD derivatives with donor-acceptor substituents.[105] The ones with *ortho* substituents have very long half-life of the quadricyclane isomer.

vealed that NBDs bearing substituents in the *ortho* positions had an extremely long half-life of the QC isomer (from about 80 days in the *meta* variation, to more than 2000 days in the *ortho*, see compounds **19**-**22** Table 3.4), without significantly compromising the other properties. Insight from theoretical calculations revealed that constrains from the steric hindrance of the *ortho* substituents induce high energetic barriers on the QC ground state energy landscape, which make the pathway to the transition state to the isomerization to NBD higher in energy. It is interesting to note how in this set of compounds, QC to NBD isomerization in the cases of *ortho* substituents have a very high positive contribution of the entropy of activation compared to their *meta* or *para* counterparts (see Table 3.4). The effect of temperature on the lifetime of QC **8**-**10** and QC **20** and **22** will be different, due to their different entropy of activation. Isomerization of QC **22** has a large positive entropy of activation, therefore its half-life is largely changing with temperature, and is expected to significantly decrease at higher temperatures, to the point where it will be shorter than the one of **20**. These two different approaches to engineering the half-life of QC derivatives by selectively affecting the enthalpy and entropy of activation can both have their advantages, and are extremely valuable tools for future designs tailored toward specific applications.

# Chapter 4

# Testing Applications and New Materials:

*In this chapter a laboratory scale device test (Paper III) is described, and observations from these experiments lead to a conversation on MOST limitations and potentials. In addition, characterisation of neat liquid MOSTs (Paper I) is presented, and new outlooks for high energy density MOST materials are analysed.*

## 4.1 Laboratory Scale Device Testing

Testing MOST materials in real devices can serve as "proof of concept", demonstrating and developing immature technologies at early stages. These kind of experiments can be very instructive for MOST, in order to identify potentials, limitations, and future challenges of promising candidates and applications. From the experiments, insights on how the technology should be developed can be gained; moreover, the efficiency of the compounds can be actually measured, and the improvements in different systems assessed. Different devices have been planned, built and tested to show the potential of MOST.[20,67,75,81,108]

It was decided, as presented in appended paper III, to investigate the potential of a hybrid technology which combines MOST and solar water heating (SWH). Even an ideal MOST is supposed to absorb only part of the solar spectrum, up to about 600 nm, but most of the existing NBDs that have overall promising properties usually have $A_{onset}$ between 350 nm and 450 nm. The idea was to make a device with an upper layer where to flow a fluid MOST (like a norbornadiene solution), and a lower layer where to flow water. In this way the incoming

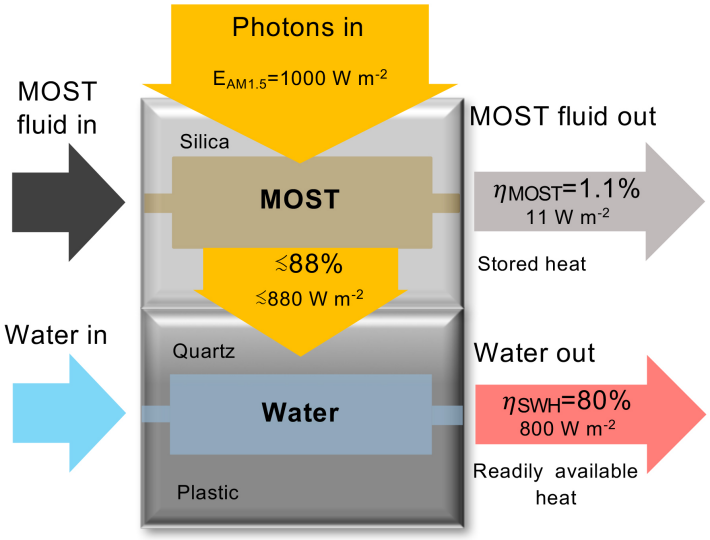


**Figure 4.1:** Illustration of a hybrid solar energy conversion device. The upper collector is used for the conversion of the MOST system; the lower collector is used for solar water heating. Measured efficiencies are reported (NBD **16** as MOST, 0.1 M in toluene, $\mathring{n}$ = 2.710-8mol s$^{-1}$, $\mathring{m}$ = 1.6 10$^{-5}$ kg s$^{-1}$). Reproduced with permission of RSC.

photons can be partially absorbed (and therefore stored) by the MOST, and the transmitted photons result in heating the water underneath. Such a technology would combine the perks of both MOST (storing heat) and SWH (readily available thermal energy with high efficiency). A device to test this concept was designed, and a schematic illustration can be seen in Figure 4.1.

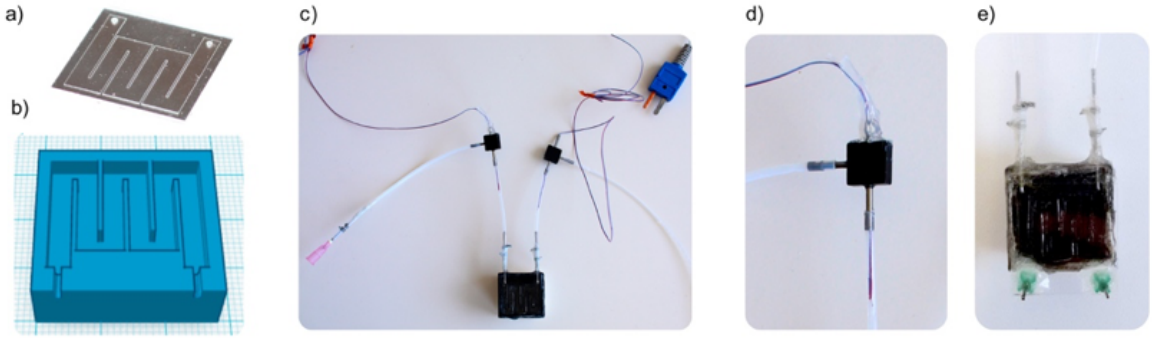


**Figure 4.2:** Planning and construction of the hybrid collector. a) Custom made quartz microfluidic chip; b) 3D model of the SWH collector; c) picture of the assembled SWH collector including connection tubes and thermocouples; d) detail of a T-junction with thermocouple; e) detail of the combined hybrid collector. Reproduced with permission of RSC.

A custom made fused silica microfluidic chip was used for the upper collector (Figure 4.2 a). It was connected with syringe needles to PTFE tubings, and a syringe pump was used to pump the solution. The lower collector (Figure 4.2 c) was made with a 3D printed winding channel (Figure 4.2 b), covered with a

quartz slide, and connected with syringe needles to PTFE tubings. In the tubings, before and after the lower collector, two thermocouples where inserted through a T-junction (Figure 4.2 d). The hybrid collector was obtained by glueing the two on top of each other (Figure 4.2 e).

To test the device the two norbornadienes **16** and **18**, shown in Figures 3.3 and 3.5 were selected. They had both been synthesised, characterised, and previously published by some of us.[81,82] The properties of **16** and **18** have partially discussed in the previous chapter. They both have a red-shifted absorption onset (389 nm and 456 nm respectively); the overlap with the solar spectrum, however, is not ideal, as can be seen in Figure 3.5 b, but the portion of sun photons absorbed is greatly increased with **16**. **18** has a good quantum yield (60%), very long $t_{1/2}$ (42.9 days), and good energy storage (86.5 kJ/mol, which could potentially give a temperature rise of about 200 °C). **16** has a much improved $A_{onset}$, but the quantum yield is unfortunately lower (28%); the energy storage is also good (103 kJ/mol), and could potentially give a temperature rise of 238 °C.

A solution of **16** and **18** in toluene (70 mM and 100 mM respectively) was circulated in the MOST collector, while irradiating it with a simulated solar radiation. The conversion of NBD to QC was then measured with $^1$H NMR. The following equation was used to calculate the solar energy storage efficiency, $\eta_{MOST}$, of the MOST system:

$$\eta_{MOST} = \frac{\dot{n}_{MOST} \cdot \alpha_{QC} \cdot \triangle H_{storage}}{A \cdot E_{AM1.5}} \tag{4.1}$$

where $\alpha_{QC}$ is the measured conversion fraction of NBD to QC after irradiation, $\triangle H_{storage}$ is the QC storage energy (in J mol$^{-1}$), $\dot{n}_{MOST}$ is the MOST flow speed (mol s$^{-1}$), $A$ is the irradiated surface, and $E_{AM1.5}$ the energy of the incoming radiation (1000 W m$^{-2}$for the AM 1.5 solar standard). $\eta_{MOST}$ of **18** and **16** was therefore calculated to be 0.1% and 1.1% respectively. These values are a great improvement compared to the previously reported MOST device test (up to 2 orders of magnitude).[20] The previously used MOST system was based on a ruthenium difulvalene derivative, which has a much lower quantum yield. These systems already represent a significant improvement of many of the key MOST properties. Moreover, a cyclability test of **16** in toluene was performed by Z. Wang and after 127 cycles the degradation was negligible demonstrating an excellent robustness.

Water was then flowed in the lower collector at different rates, while irradiating under simulated sun conditions. A the same time, in the MOST collector, air, or toluene, or **18** or **16** in toluene solutions were circulated, to investigate the effects

of these on the performance of the SWH device. The efficiency of the solar water heating collector $\eta_{SWH}$ was then calculated according to the following equation:

$$\eta_{SWH} = \frac{\dot{m}_{H_2O} \cdot C_{PH_2O} \cdot \triangle T}{A \cdot E_{AM1.5}} \tag{4.2}$$

where $\dot{m}_{H_2O}$ is the flow rate of the water (Kg $s^{-1}$), $C_{PH_2O}$ is the heat capacity of water (J $Kg^{-1}$ $K^{-1}$), $\triangle T$ is the measured temperature increase (K). The measured $\triangle T$and $\eta_{SWH}$ at the different flow rates are in Figure 4.3. The thermal behaviour of the device was also simulated (the simulation was performed by K. Börjesson), giving a good agreement with the experimental data. It is shown that the presence of the MOST does not significantly affect the performance of the SWH collector. The simulation was also used to predict the efficiency $\eta_{SWH}$ when an optimised norbornadiene (with an onset of absorption of 590 nm)[26] is used in the MOST collector. In this case $\eta_{SWH}$ is more affected by the MOST layer which absorbs a significant part of the incoming light, but it is calculated that the total efficiency of the device will be still higher respect to the SWH device alone (see attached Paper III).

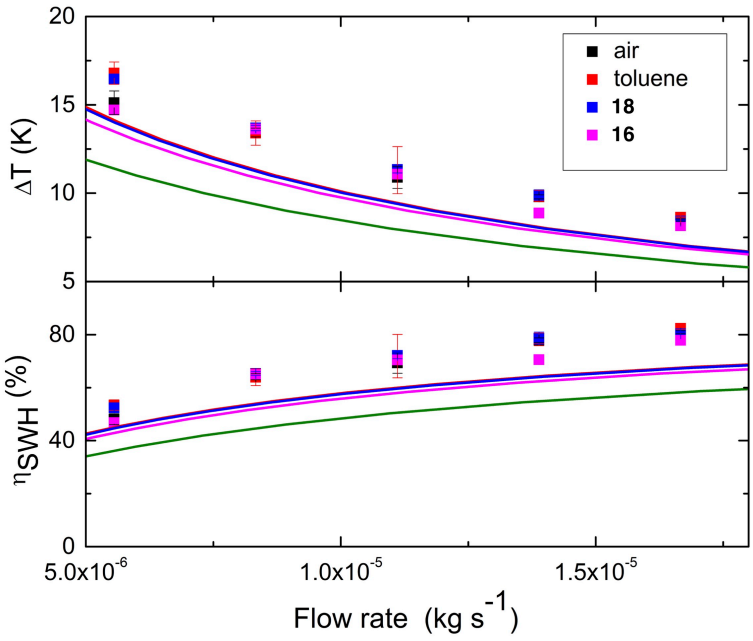


**Figure 4.3:** Increase of water temperature and SWH at different flow rates. In the upper collector air (black), toluene (red), **18** (blue) or **18** (pink) in toluene were circulated; errors as standard deviations are reported for the measurements done while in the upper collector is circulating air, toluene or **18**. The measured points are compared with the simulated values (solid lines, same colour coding). The device operating with an optimised MOST system with cut off at 590 nm is also simulated (green line). Image reproduced with permission of RSC.

An evaluation of the different energy losses competing to the efficiency $\eta_{MOST}$ was done. Part of the energy is lost because of the poor spectral overlap with the sun spectrum. This can be improved by red-shifting the NBD absorption or by utilising the transmitted photons, as suggested here, to heat water. Of the absorbed energy, part of it is not stored due to inefficient photoisomerization process, and in **16** this loss equals to 72%; highlighting the significance of this property on the storing efficiency of a MOST system. This loss parameter, $E_{iso}$, can be calculated as follows:

$$E_{iso} = \int_0^{\lambda_{onset}} n_f \cdot E_f \cdot (1 - \phi) d\lambda \tag{4.3}$$

where $n_f$ is the photons flow in the solar spectrum at each wavelength (in $s^{-1}$ $m^{-2}$ $nm^{-1}$) and $E_f$ is the energy of each photon (in J $nm^{-1}$).

Some energy is also lost when the excited NBD undergo radiationless relaxation to a local minimum and then photoisomerise to the QC, this parameter, $E_{relax}$, is calculated as:

$$E_{relax} = \int_0^{\lambda_{onset}} n_f \cdot (E_f - \frac{\triangle H_{storage}}{N_A}) \cdot \phi d\lambda \tag{4.4}$$

where $N_A$ is the Avogadro´s number. This loss parameter include also part of the energy that is used for the barrier to the back isomerization.

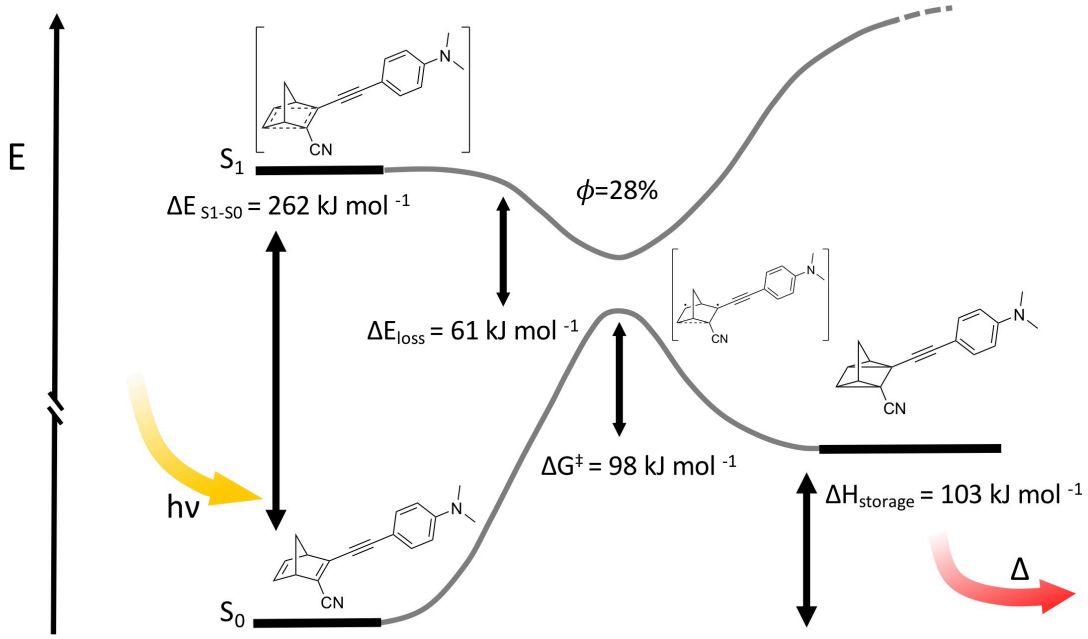


**Figure 4.4:** Energy scheme of **16** with reported the measured values. $\triangle G^{\ddagger}$ is calculated at 25 ℃.

If we look more in detail at **16** in Figure 4.4, the energy difference between NBD and its excited state $S_1$is 262 kJ mol$^{-1}$ (calculated from the measured absorption spectrum), and $\triangle H_{storage}$ was measured to be 103 kJ mol$^{-1}$. Of their difference, which equals to 159 kJ mol$^{-1}$, at least 98 kJ mol$^{-1}$ are used to accommodate the activation energy barrier (this is the $\triangle G^{\ddagger}$ at 25 °C), and leaves about 61 kJ mol$^{-1}$ of losses which will most likely result in heating of the MOST medium. This energy gap could be hypothetically decreased if the vibrational relaxation on $S_1$ and its energy difference with $S_0$ were minimised. Except "trial and error", supported by theoretical modelling, there are to date no strategies for minimising the energy difference between the excited state of NBD and QC to the amount of energy needed for a reasonable barrier to the back isomerization, without compromising other properties as the $A_{onset}$ and $\triangle H_{storage}$.

Other fundamental aspects emerged from these proof of concept experiments; for example NBDs **16** and **18** are solid compounds at room temperature, which have been diluted in toluene. Dilution obviously decrease the energy storage density, and needs to be taken into account. Dilution is mostly needed in order to perform characterisations, but has to be reduced or removed to make high energy density operational MOST materials.

## 4.2 Developing new Norbornadienes Based Materials for MOST

MOST materials that are developed based on norbornadiene derivatives should be solid or liquid. NBDs have been previously added to polymers, and they were able to switch between the isomers, maintaining an impressive robustness over thousands cycles.[63] Liquid, neat norbornadienes are of great interests since they could be used in closed system flow devices, but had never been made or tested before. Neat NBDs **3a**-**d** have very promising properties in solution, moreover they are all liquid at room temperature. Their shear viscosity was measured and it is between 0.03 and 0.07 Pa s, which is comparable to the one of colza oil (see Figure 4.5).

A thin layer of neat NBDs was obtained by putting a drop of each in between two microscope glass slides. The samples prepared in this way could be inserted in a spectrophotometer and also irradiated. After irradiation with LEDs (365 nm), the absorption band decreased, which is typically correlated with the photoisomerization to QC ( see Figure 4.6 a). The absorption at 355 nm was then followed over time at room temperature, and it increased following an exponen-

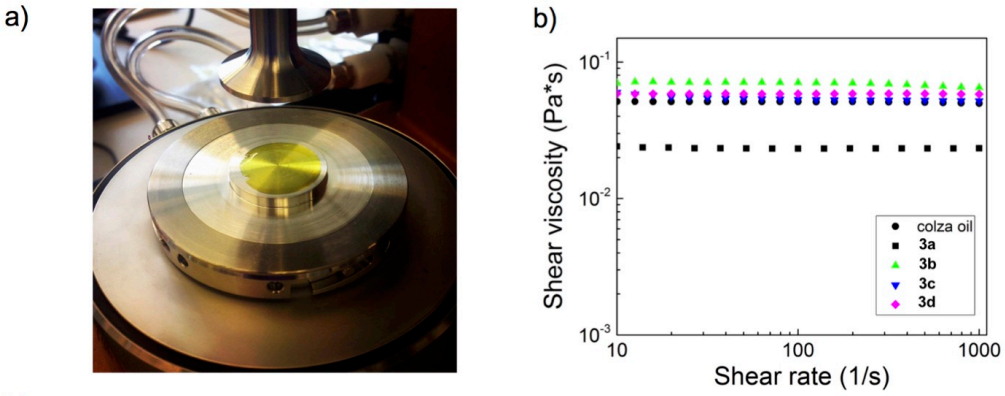


**Figure 4.5:** a) Picture of about 300 $\mu$l of liquid NBD **3a** in the rheometer. b) Measured shear viscosity of **3a**-**d** and colza oil. Reproduced with permission of Wiley.

tial curve, confirming a first order kinetic process (Figure 4.6 b). The measured QC half-life gave variable results, which was suggested could be due to the difficulty of controlling the temperature in this experimental set-up. Although degradation or other effects (for example the influence of slides thickness) could not be totally excluded. Even more surprisingly, the measured $t_{1/2}$ fall within the range of minutes, which is much shorter than the values measured in solutions. It was therefore speculated that microscopic phenomena of local heat release were facilitating the thermal isomerization. Moreover, a change in medium (in this case from solvent to neat) could potentially also affect the transition state or the mechanism, but these are only hypothesis as for now. Future studies should investigate NBD derivatives with different donor-acceptor groups, and also the eventual effect of dilution in highly concentrated samples.

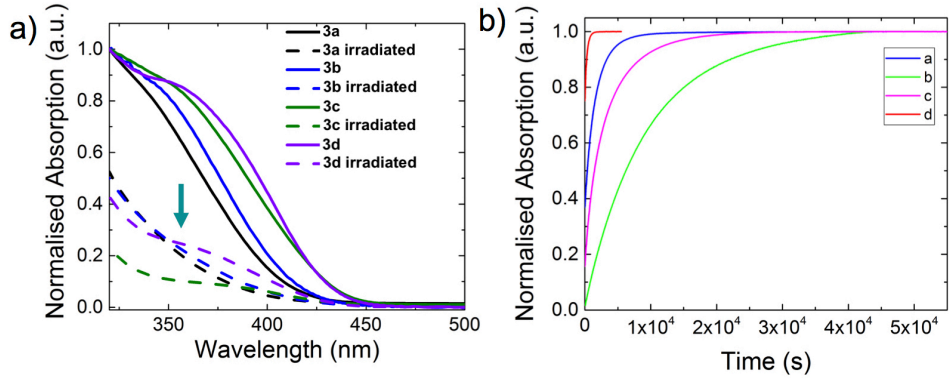


**Figure 4.6:** a) Decrease of the absorption band is observed after irradiation (365 nm) of neat samples of **3a** - **d**. b) After stopping the irradiation, the absorption (measured at 355 nm) increases over time at room temperature. Reproduced with permission of Wiley.

An interesting difference between solutions and neat samples was the sta-

bility toward repeated cycles of NBD to QC photoisomerization and back conversion. Samples dissolved in solutions exhibited relatively good stability toward multiple isomerization cycles even without degassing the solution. Neat samples instead showed a significant degradation during the first cycle (about 60%), and small degradation during the subsequent cycles, as seen in Figure 4.7. Using radical stabiliser or removing oxygen from samples of **3a** did not seem to improve the stability during the first isomerization cycle. NMR of the samples after the degradation show the appearance of broad peaks which could be correlated to formation of polymeric byproducts. Based on the observed degradation it seems that even a small dilution of the samples, or other strategies to interfere with intermolecular reactions, could potentially significantly improve their stability.

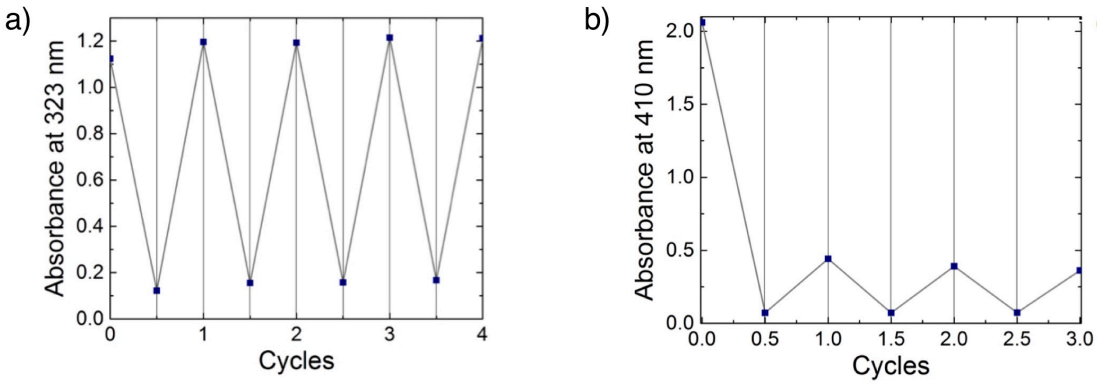


**Figure 4.7:** Absorption measured at 323 nm of a toluene solution of **3a** undergoing multiple cycles of irradiation (365 nm) and thermal back conversion (above 60℃). b) Absorption measured at 410 nm of a neat thin film of **3a** undergoing multiple cycles of irradiation (365 nm) and back isomerization at room temperature.

# Chapter 5

# Summary of Significant Achievements and Outlooks

A simple, scalable, and efficient synthesis toward donor-acceptor norbornadienes have been identified. The synthesized series of donor-acceptor norbornadienes (**3a**-**d**) have overall good properties, with well red-shifted $A_{onset}$, $t_{1/2}$ of about 100 hours that would suit day to night storage applications, high quantum yield, and high energy density for low/medium heat applications. An efficient way to control the kinetic stability of QCs by engineering the entropy of activation have been rationalised. This is based on the introduction of bulky iPr groups on the bridge (C7) position of NBDs; their rotation is more sterically hindered in the NBD isomers, and less in the QCs. The gained insight into the mechanism of the back isomerization is of great value for designing future MOST systems with long storage times. A laboratory scale microfluidic device have been designed, built, and used to test a hybrid technology combining MOST with solar water heating. Testing it demonstrated how combining these technologies would lead to an overall higher total efficiency and performance. Moreover, these experiments helped identifying new challenges to be faced in the future development of MOST technologies. The importance of high quantum yield of photoisomerization, and functional high energy density materials were therefore highlighted. The properties of the synthesized norbornadienes (**3a**-**d**) which are liquid at room temperature have been tested in neat samples. The liquid NBDs pohotoisomerised and back-converted in neat samples, but new challenges emerged. Future research will have to aim for longer half-life of QCs in neat, or highly concentrated samples, and improve the stability over multiple cycles of photoisomerization and back conversion.

The work presented in this thesis has been part of a larger project, where team efforts allowed to reach many remarkable results. The MOST technology is still at a research level but significant advancements were achieved in the last years.Some of the most noteworthy results by the MOST team colleagues are for example innovative NBDs oligomers with dimeric or trimeric structures.[?] These exhibit red-shifted absorption (up to above 400 nm), in most cases high $\phi$ (up to 94%), and high energy storage density (measured up to about 600 kJ mol$^{-1}$). As previously discussed, a way to reach outstanding improvements in storage time has been discovered by Jevric *et al.* in donor-acceptor NBDs with aromatic groups bearing *ortho* substituents.[105] Wang *et al.* managed to measure the microscopic heat released by the catalysed conversion of a quadricyclane derivative to the norbornadiene isomer, with observed $\triangle T$ up to 63 °C.[109]

Future work will have to address challenges that are still unresolved. It emerges from the work in this thesis how the strategy to extend the storage times and improve $\phi$ in Paper II could be applied to existing molecules to improve their features (for example **16**). More work needs to be invested into developing neat or highly concentrate operational liquid or solid MOSTs. Defined applications need to be clearly identified, and the goal properties have to be stated. Device testing will play a crucial role in this phase. Devices to test the full cycles of photoisomerization and catalysed backconversion will be particularly interesting in assessing MOST technologies, and developing efficient catalysts. New compounds with overall optimised properties toward the selected applications need to be identified, and it is fundamental to develop efficient syntheses and scale them up. Scaling up plays a vital role also in device testing (more material is often needed in that case), safety assessment, and costs evaluation; these are very important goals in order to achieve real applications. To exploit the potential of NBD-QC systems and technologies such as MOST, not only basic research, but more significant collaborations with industries and agencies are needed. It is believed by the author of this thesis that it will be these precious collaborations that will allow to fill the gap with the “ivory tower” that is university research. It will be exciting to see what the future will bring.

Norbornadienes are very versatile systems, and derivatives have been investigated not only for MOST, but also for a diverse range of applications. Examples of other potential applications are as switches for molecular electronic applications,[110] optoelectronic,[111,112] data-storage,[113] and chemosensors.[114] While being immersed in working toward efficient MOST systems, it has been also important to not forget how university research is in many cases a wonderfully free environment. Original ideas, collaborations, side tracks, and serendipitous dis-

coveries can still some times find place to happen and grow. Historically, they have often brought amazing and impactful discoveries and are key to identification of potential new applications. It is important, while dutifully pursuing our main research objectives, to not forget about keeping our minds open and playful, chase fun ideas, and enjoy serendipity. The next chapter will present one of these enjoyable and fruitful “side-tracks”.

# Chapter 6

# A Versatile Norbornadiene: Exploring New Applications in Molecular Logic

*In this chapter the field of molecular logic is briefly introduced. A norbornadiene based molecular keypad lock is demonstrated (Paper IV).*

Molecular logic is an interdisciplinary field based on the concept of using intrinsic features of molecular systems to perform logic operations. While traditional silicon based logic elements are voltage dependent, molecular switches and systems can, upon receiving chemical or photonic inputs, become distinct species with specific physical properties as outputs. It was suggested to use these systems to perform Boolean logic operations and process information at a molecular level. De Silva published in 1993,[115] a molecule that can bind hydrogen and sodium ions. It gives different fluorescence signals depending on the ions concentration, with high intensity fluorescence only when both ions are above a certain concentration. This system works in fact as an AND logic gate. During the years the field developed and attracted a lot of attention. Systems utilising different chemical and physical signals as inputs and outputs (such as pH, redox agents, ions, light, temperature and more) have been demonstrated as logic gates.[116–120] One of the big challenges have been concatenation of logic gates into larger systems with more advanced functionalities, and photochemical processes have been the favourited choice because of their efficiency and lack of chemical byproducts.[121,122] The idea of making molecular based computers hampered over the years due to intrinsic difficulties, and new ways to

use the complex functionalities of these systems have been explored. Molecular logic systems have been investigated for example for drug release, drug activation and sensing, and other advanced applications.[123–125] One of the suggested use is for security measures, to encrypt and protect sensitive data, and in the past different switches or more complex molecular systems have been investigated as keypad locks. In these systems a combination of inputs, applied in a specific order (a "key") gives a unique output.[126–128] Different molecular photoswitches have been investigated for this application, and molecules undergoing photoinduced processes are in general the preferred choice for the above mentioned reasons.[121,126,129–133] To the best of our knowledge, norbornadiene-quadricyclane photoswitches had never been investigated for molecular logic or security applications before.

## 6.1 A Norbornadiene-Quadricyclane Based Molecular Keypad Lock

Norbornadiene-quadricyclane **16** is a versatile molecular photoswitch which, as discussed in the previous chapters, has very promising features for MOST application.

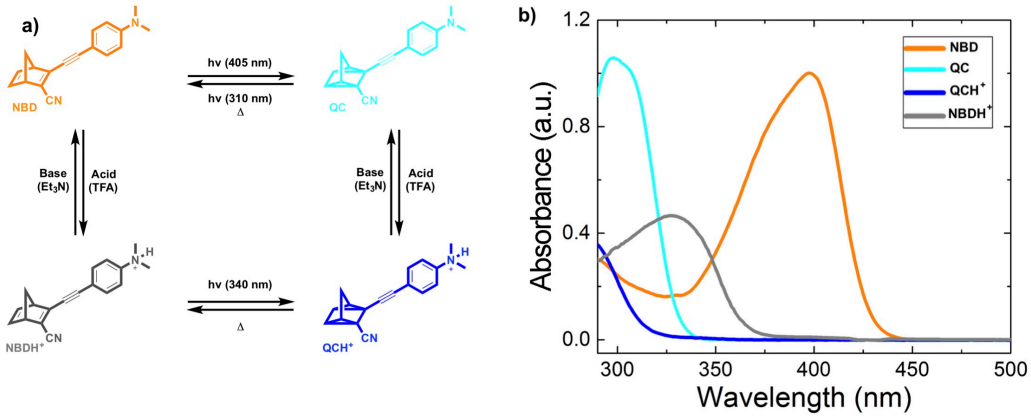


**Figure 6.1:** a) Interconversion scheme between the four species $NBDH^+$, NBD, QC, and $QC^+$. b) Spectra of the four species, measured in toluene solution.

It is simply and efficiently synthesised from the commercially available NBD in just 3 steps. Due to the presence of the donor and acceptor groups on the double bond, the absorption of NBD **16** is red-shifted with an onset of about 450 nm. Upon photoisomerization the double bond between the donor and acceptor groups is converted to a single bond, breaking the conjugation and therefore blue-shifting the absorption of QC **16** down to 344 nm. NBD **16** photoisomerise

to QC **16** upon irradiation between 375 and 450 nm ($\phi$ = 28% measured at 410 nm). Interestingly, it was observed by colleagues Z. Wang and B. E. Tebikachew how irradiation of QC **16** with light at 310 nm would induce photoisomerization back to NBD **16**, with $\phi$ = 53% measured at 300 nm. Photoisomerization of QC to NBD upon irradiation with deep UV light has been observed before (in NBD moieties incorporated into polymers) but this feature is rarely observed.[77,78] In this case, it allows **16** to be used for applications where fast (< 1 min) interconversion between NBD and QC isomer is required. Another interesting feature of **16** is the methylated amino group, which can be protonated. It was predicted how protonation of the amino group would decrease it electron-donating character, disrupting the push-pull system. This would in turn further blue-shift the absorption spectra in the protonated forms ($NBDH^+$ and $QCH^+$ seen in Figure 6.1), which was in fact observed (Figure 6.1 b).

It is possible to observe in Figure 6.1 how **16** (in toluene solution) can interconvert between 4 different species, each of them with a distinct absorption spectrum. NBD **16** as an absorption maximum at about 405 nm; it can be protonated to $NBDH^+$ **16** (which has an absorption maximum at about 330 nm) by addition of acid (for example trifluoroacetic acid TFA). The deprotonation back to NBD **16** proceed readily by adding a base (such triethylamine $Et_3N$). NBD **16** can be readily photoisomerised to QC **16** (which has a high absorption maximum at about 300 nm, and onset at 344 nm) by irradiation at 410 nm. The back conversion to NBD **16** occurs thermally (time constant of about 7 h at 25 °C in toluene) or, as we have seen, photochemically (irradiation at 300 nm). QC **16** can also be protonated to $QCH^+$ **16**, which has a very blue shifted spectrum with onset at around 320 nm, by addition of an acid such as TFA. Deprotonation back to QC **16** can be accomplished by adding a base such as $Et_3N$. Irradiation of $NBDH^+$**16** at 340 nm showed partial decrease of the absorption band usually associated with photoisomerization. $QCH^+$**16** thermally convert to $NBDH^+$**16** with a time constant of about 2.5 h at room temperature in toluene solution, but some degradation is also observed in this process. More importantly, due to its spectral features (the absorption is extremely blue-shifted), and also to the solvent cut-off, it is not possible to photoisomerise it back to $NBDH^+$**16**. The photoinduced isomerisation proceed usually efficiently within a minute of irradiation with LEDs of appropriate wavelength (and power between 25–870 mW), while within this time scale the thermal isomerisations are minimal. The interconversions between the four states of **16** are well understood and their properties rationalised. It was therefore suggested in appended Paper IV to exploit this system for making a three-input molecular keypad lock. The three inputs are: (a) acid, (b) base, and

(UV) light at 310 nm. $QCH^+$**16** is chosen as the initial state. Looking at the interconversion scheme, it is evident that there is only one way to make $NBDH^+$**16** from $QCH^+$**16**, which is to apply the inputs in the following sequence: b, UV, a. $NBDH^+$**16** has a characteristic absorption maximum at 330 nm; the measured absorbance at 330 nm is chosen as output, and needs to be high in order to "open the lock". All the possible combinations of inputs are listed in Table 6.1, and the predicted formed species are in Table 6.2. All the input sequences were tested on toluene solutions of $QCH^+$**16** (which was formed *in situ* from the synthesised NBD **16** by irradiation at 405 nm and protonation with TFA), and the spectra after each input were recorded recorded. The absorption spectra were read at the output wavelength of 330 nm, and as expected only sequence 4 gave an absorbance higher than the threshold, here set at $A = 0.25$ (see Figure 6.2). Reading the absorbance at 310 nm or 405 nm (Figure 6.2 b and c) gives the information if QC or NBD have been formed as predominant specie, and the results reflect the expected ones from Table 6.2.

**Table 6.1:** Possible permutations of the three inputs: acid (a), base (b), 310 nm light (UV).

| 1 | 2 | 3 | 4 | 5 | 6 | 7 | 8 | 9 | 10 | 11 | 12 | 13 | 14 | 15 |
|---|---|---|---|---|---|---|---|---|---|---|---|---|---|---|
| a | a | b | b | UV | UV | a | b | a | UV | b | UV | a | b | UV |
| b | UV | a | UV | a | b | b | a | UV | a | UV | b | | | |
| UV | b | UV | a | b | a | | | | | | | | | |

**Table 6.2:** Species that are expected to form when a $QCH^+$ toluene solution is subjected to each of the possible combinations of the three inputs a, b and UV. Only combination 4 forms $NBDH^+$.

| 1 | 2 | 3 | 4 | 5 | 6 |
|---|---|---|---|---|---|
| $QCH^+$ | $QCH^+$ | $QCH^+$ | $QCH^+$ | $QCH^+$ | $QCH^+$ |
| $QCH^+$ | $QCH^+$ | QC | QC | $QCH^+$ | $QCH^+$ |
| QC | $QCH^+$ | $QCH^+$ | NBD | $QCH^+$ | QC |
| NBD | QC | $QCH^+$ | $NBDH^+$ | QC | $QCH^+$ |

| 7 | 8 | 9 | 10 | 11 | 12 | 13 | 14 | 15 |
|---|---|---|---|---|---|---|---|---|
| $QCH^+$ | $QCH^+$ | $QCH^+$ | $QCH^+$ | $QCH^+$ | $QCH^+$ | $QCH^+$ | $QCH^+$ | $QCH^+$ |
| $QCH^+$ | QC | $QCH^+$ | $QCH^+$ | QC | $QCH^+$ | $QCH^+$ | QC | $QCH^+$ |
| QC | $QCH^+$ | $QCH^+$ | $QCH^+$ | NBD | QC | | | |

The performed experiment demonstrates how this system could conceptually work as a molecular keypad lock. There are also some drawbacks, for example chemical inputs are not the best choice, especially if it is expected to use the system over multiple cycles, because of the formation of byproduct. All-photonic

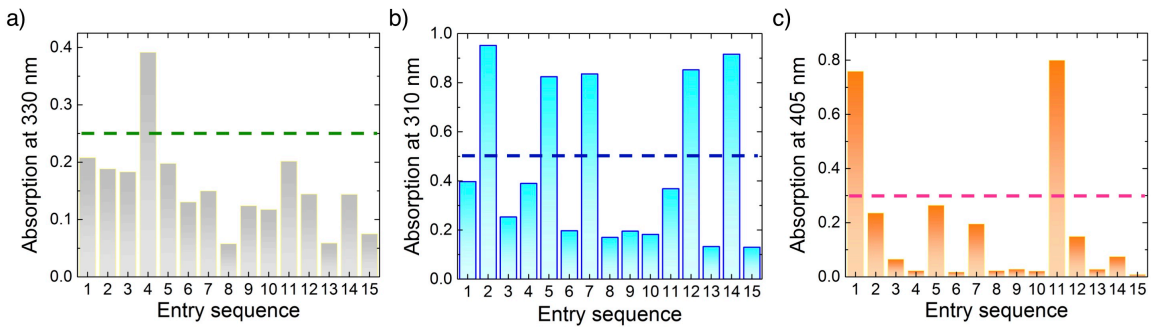


**Figure 6.2:** a) Output reading of the absorption at 330 nm of the final species after applying sequences 1-5 to a toluene solution of $QCH^+$. The absorption after sequence 4 is the only one above the threshold level, arbitrarily set at A = 0.25. By reading the absorptions at 310 nm (b) or 405 nm (c), it is possible to identify if QC (sequences 2, 5, 7, 12, 14) or NBD (sequences 1, 11) have been formed.

systems are preferred and should be the first choice in future molecular logic applications. Moreover, a three input, 15 sequences lock is not highly secure, and would likely not be useful for real safety applications. Still, it is the first known example of a NBD-QC based molecular logic element, and it will hopefully attract more interest on these systems in the future. NBD-QC based photoswitches are extremely versatile systems, with a vast library of easy to synthesise derivatives. Their properties are well understood and change within a wide range of values. Therefore, it is believed that they have a great potential as molecular logic elements, and also for new and diverse applications.

# Chapter 7

# Methods

This chapter is intended to very briefly illustrate some of the concepts and theory behind the methods used in the work presented in this thesis.

## 7.1 Optical spectroscopy

When a molecule interacts with light many different processes may occur. Light-matter interactions can be described with a so-called a Jablonski diagram (in Figure 7.1). When a molecule absorbs light with an appropriate energy, an electron will be promoted to a higher energy level, and the molecule will be in an excited state. The excited molecule can then undergo different processes, of which the main ones can be summarised in radiationless vibrational relaxations, internal conversion or intersystem crossing (see Figure 7.1). Moreover the absorbed energy can be emitted through fluorescence or phosphorescence.

A useful characterisation technique consists into measuring the absorption of light in the UV-Vis range, meaning between 200 and 800 nm. Whit an UV-Vis spectrophotometer it is possible to measure the absorbance, defined as:

$$A = log_{10}\left(\frac{I_0}{I}\right) = -log_{10}T \tag{7.1}$$

where $A$ is the measured absorbance, $I_0$ is the intensity of the incident light, $I$ is the intensity of the transmitted light, and $T$ the transmittance.

From the absorbance it is possible to calculate the molar absorptivity $\varepsilon$ using the Lambert - Beer law:

$$A = \varepsilon lc \tag{7.2}$$

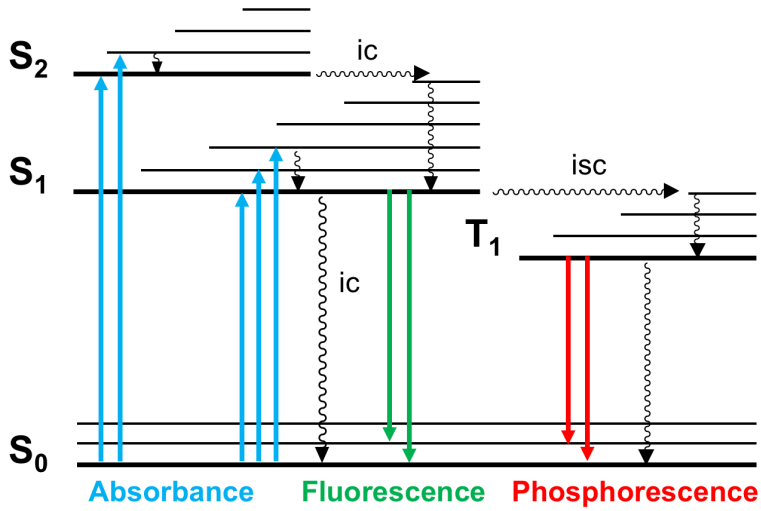


**Figure 7.1:** Jablonski diagram. Thick black lines indicate electronic energy levels, thin black lines indicate vibronic energy levels. Blue arrows indicate absorbance of light, green arrows are for fluorescence emission, red arrows phosphorescence emission. Ondulated arrows indicate radioationless transitions, *ic* is internal conversion and *isc* intersystem crossing.

where $l$ is the path length of the light through the material and $c$ the concentration. This relationship is valid in a wide range of diluted organic solutions, and it is extremely useful since it correlates the concentration to the mesured absorbance in a linear way. UV-Vis absorption spectroscopy is a versatile technique which allows to determine the exact concentration of the absorbing species in solution, and to follow eventual variations of this concentration with very high sensitivity. It is valid only for diluted solutions, therefore it will deviate form linearity when concentrations become very high. Deviation from linearity or change in intensity can also indicate the presence of more than a specie in solution, or changes to the solute composition .

### 7.1.1 Kinetics of the Thermal Isomerization

The compounds that have been studied in this thesis absorb light in the ultravioelt-visible range. Upon exposure to light, the compounds photoconvert to the quadricyclane isomer, and the absorption of the latter is significantly blue-shifted (since the conjugation through the double bond is broken).

This property can be exploited to follow conversion between NBDs and QCs. Specifically, it is of value to measure the kinetics of the thermal back isomerization of quadricyclanes to norbornadienes. Typically the quadricyclane solution is prepared *in situ* by irradiation, and the absorption at a specific wavelength and temperature is then followed over time. The thermal isomerization of QC to NBD

follows a first order kinetic, therefore the measured curve can be fitted to a first order exponential function, to obtain the rate constant ($k$) for the process. Knowing the rate constants at different temperatures ($T$) it is possible to calculate the enthalpy and entropy of activation ($\triangle H^{\ddagger}$ and$\triangle S^{\ddagger}$ respectively) using the linear form of the Eyring-Polanyi equation:[106,107]

$$ln\frac{k}{T} = \frac{-\triangle H^{\ddagger}}{R} \cdot \frac{1}{T} + ln\frac{k_B}{h} + \frac{\triangle S^{\ddagger}}{R} \tag{7.3}$$

where $R$ is the gas constant, $k_B$ is the Boltzmann constant, $h$ is the Planck´s constant.

Since the process follows a first order kinetic, the half life $t_{1/2}$ (defined as the time where the concentration is decreased by half) can be easily calculated. It simply depends from the rate of the reaction and the natural logaritm of 2, according to the following equation:

$$t_{1/2} = \frac{ln2}{k} \tag{7.4}$$

### 7.1.2 Photoisomerization Quantum Yield

UV-Vis absorption spectroscopy is also the chosen tool to characterise the efficiency of the NBD to QC photosomerization. The theory and methods for determining the photoisomerization quantum yield of photoswitches used in the work presented in this thesis is the same as described in a previously published work.[134]

In a generic system with two molecule A and B, different photo and thermally induced processes can occur, as described in Figure 7.2. These include photoisomerization of A to B (blue arrow in figure), photoisomerization of B to A (green arrow), and thermal conversion from B to A (red arrow). The equation which describe the the rates of these processes is:[134]

$$\frac{dA}{dt} = -\frac{\phi_A \cdot I \cdot \beta_A(t)}{N_A \cdot V} + \frac{\phi_B \cdot I \cdot \beta_B(t)}{N_A \cdot V} + k_{t,B\rightarrow A}\,[B] \tag{7.5}$$

where $\phi_A$ and $\phi_B$ are photoisomerization quantum yield of A and B respectively, $I$ is the photon flux of the light source, $\beta_A$ and $\beta_B$ are the fractions of photons absorbed by A and B respectively, $N_A$ is Avogadro´s number, $k_t$ is the rate constant for the thermal back conversion, V the volume of the sample, and $[B]$ the concentration of B.

In this thesis, the used method assumes a total absorption regime. In this

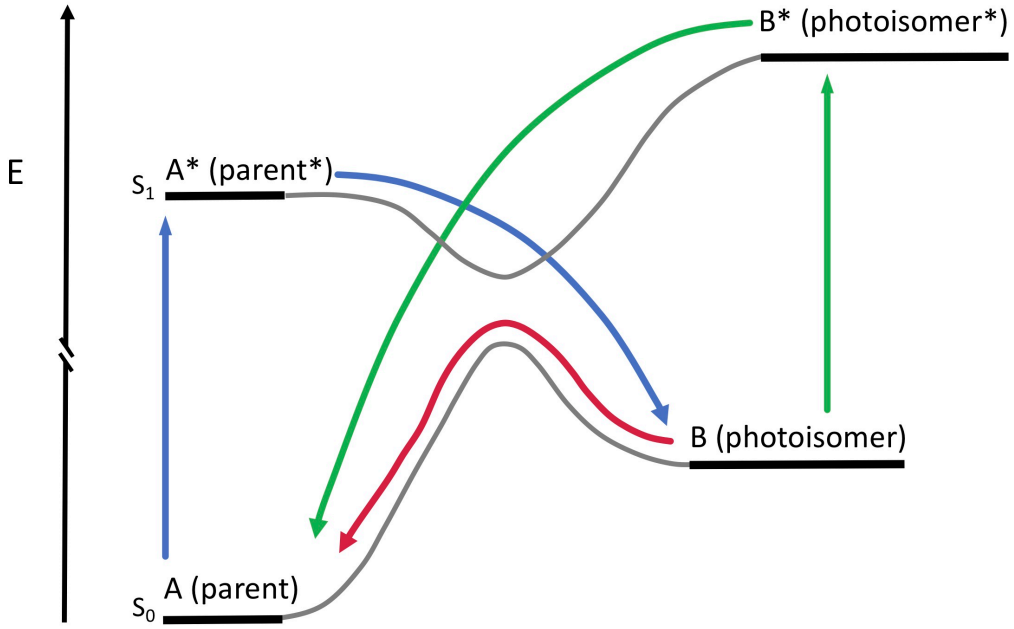


**Figure 7.2:** Simplified energy scheme of a molecular system undergoing photo and thermally induced processes between isomers A and B. Blue arrow follow the photoisomerization of A to B while green arrow show the photoisomerization of B to A. Red arrow indicates the thermally driven conversion of B to A.

condition, the absorbance of A at the irradiation wavelength is above 2 during the experiment, therefore at least 99% of the photons are absorbed. Moreover, the absorbance and thermal isomerization of B are negligible at the chosen experimental conditions. Therefore in this specific case it can be safely assumed that the photoisomerization of A to B is the main process occurring. After irradiating the B containing solution for a certain time $t_{irr}$, an amount of A will be formed. By using the Lambert-Beer equation (see eq. 7.2) to correlate the concentration of A in solution to its measured absorbance, equation 7.5 can be simplified and integrated to give:[134]

$$[A] = [A_0] - \frac{\phi_A \cdot I}{N_A \cdot V} \cdot t_{irr} \tag{7.6}$$

It is of course necessary to know the photon flux of the light source, which should be monochromatic and with a collimated beam. To determine the photon flux, chemical actinometry was used. A compound which undergoes a photochemical process with a known quantum yield is used as a reference standard to determine the photon flux. In the present work, a modified version of the previously published ferrioxalate actinometry[135] was used. It is based on the photochemical degradation of ferrioxalate, which was chosen because of the reliability

of the given results:

$$Fe(C_2O_4)_3^{3-} \xrightarrow{h\nu} Fe^{2+} + C_2O_4^{\cdot -} + 2C_2O_4^{2-} \tag{7.7}$$

$$Fe(C_2O_4)_3^{3-} + C_2O_4^{\cdot -} \xrightarrow{\triangle} Fe^{2+} + C_2O_4^{\cdot -} + 2CO_2 + C_2O_4^{\cdot -} + 3C_2O_4^{2-} \tag{7.8}$$

The method for measuring the photon flux in this way is described more in detail in a recently published work.[134]

The set up of the quantum yield measurement has been recently improved in the group. It consists of a UV-Vis spectrophotometer equipped with a four way cell holder, that has also a temperature controller and the possibility to apply stirring. In this way it is possible to irradiate and monitor the solution at the same time. Collimated diodes of the appropriate wavelength were controleld manually or using a computer controlled trigger, programmed to irradiate the sample for defined time intervals. After each irradiation the UV-Vis spectra were recorded. By doing a linear fitting of the measured absorption after different irradiation times, and using equation 7.6, it is possible to calculate the quantum yield.

## 7.2 NMR Study of Dynamic Processes

Basic knowledge of the theory behind nuclear magnetic resonance (NMR) spectroscopy is assumed as known. Variable temperature experiments to study dynamic processes in the molecular systems have been conducted in the work presented in this thesis. The theory behind them is very briefly presented.

Dynamic processes can be faster or slower in respect to the NMR measuring time scale. In the first case the measured signals result from an average of the conformations the atoms have occupied during the experiment time. In the second case different signals are measured for the different conformations occupied by the atoms, as can be seen in Figure 7.3. By changing the temperature the dynamic processes will of course occur faster or slower. At a temperature where the speed of the processes is intermediate, a broad signal is observed, and it is said to have coalescence.[136] If the processes are slow enough on the NMR scale, the signals could also give cross peaks due to chemical exchange in a NOESY experiment. In this type of experiment the signal due to NOE effect will have the opposite sign with respect to the diagonal of the spectrum, while signals due to chemical exchange will have the same sign. In this way it is possible to distinguish the two different types of cross peaks, and further confirm the peaks

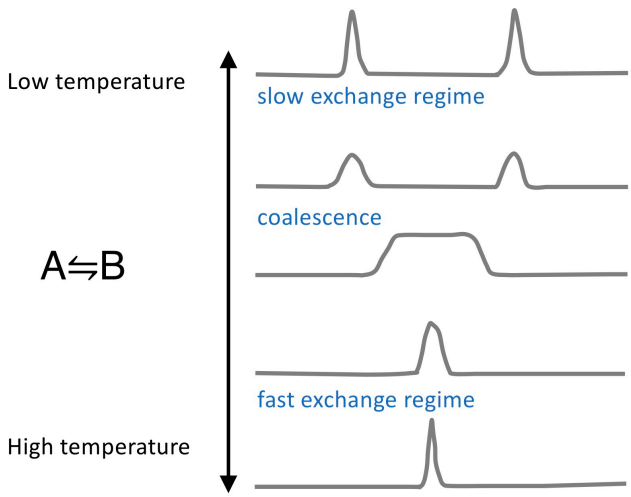


**Figure 7.3:** Expected NMR spectra of a molecular system interconverting between two conformations A and B each giving different signals.

that are eventually associated to the same nuclei.

## 7.3 Differential Scanning Calorimetry

Differential scanning calorimetry is a thermoanalytical technique. It measures how much energy is required to heat a sample at a certain temperature compared to a reference. If the sample is undergoing an endothermic process it will need more power than the reference; if it undergoes an exothermic process then it will need less power than the reference to reach the same temperature. DSC is mainly used to determine energetics of phase transitions.

In the work presented in this thesis, the observed process is the thermal isomerization of quadricyclanes to norbornadienes. This process can be induced by heating, and it is accompanied by heat release. By knowing the exact amount of material in the DSC sample it is possible to normalise the measured heat release, and to calculate the enthalpy difference between the quadricyclane and norbornadiene isomer. This correspond to the energy storage density of the MOST system.

# Bibliography


1. IPCC, *Climate Change Synthesis Report Summary for Policymakers*; 2014.

2. UN FCCC Conference of the Parties (COP), *ADOPTION OF THE PARIS AGREEMENT*; 2015.

3. Rogelj, J.; den Elzen, M.; Höhne, N.; Fransen, T.; Fekete, H.; Winkler, H.; Schaeffer, R.; Sha, F.; Riahi, K.; Meinshausen, M. *Nature* **2016**, *534*, 631–639.

4. Sokolov, A.; Paltsev, S.; Chen, H.; Monier, E. *Geophysical Research Abstracts* **2016**, *18*, 8016.

5. Victor, D. G.; Akimoto, K.; Kaya, Y.; Yamaguchi, M.; Cullenward, D.; Hepburn, C. *Nature* **2017**, *548*, 25–27.

6. IRENA, *Renewable Energy: A key climate solution*; 2017.

7. IRENA, *Global Energy Transformation - A Roadmap to 2050*; 2018.

8. IEA International Energy Agency, *Technology Roadmap Solar Thermal Electricity*; 2014.

9. Green, M. A.; Ho-Baillie, A.; Snaith, H. J. *Nature photonics* **2014**, *8*, 506–514.

10. Li, G.; Zhu, R.; Yang, Y. *Nature photonics* **2012**, *6*, 153–161.

11. Wolden, C. A.; Kurtin, J.; Baxter, J. B.; Repins, I.; Shaheen, S. E.; Torvik, J. T.; Rockett, A. A.; Fthenakis, V. M.; Aydil, E. S. *Journal of Vacuum Science & Technology A: Vacuum, Surfaces, and Films* **2011**, *29*.

12. Hardin, B. E.; Snaith, H. J.; McGehee, M. D. *Nature photonics* **2012**, *6*, 162–169.

13. Pandey, A. K.; Tyagi, V. V.; Selvaraj, J. A. L.; Rahim, N. A.; Tyagi, S. K. *Renewable and Sustainable Energy Reviews* **2016**, *53*, 859–884.

14. Balzani, V.; Credi, A.; Venturi, M. *Photochemical Conversion of Solar Energy*; 2008; pp 26–58.

15. Armaroli, N.; Balzani, V. *Angewandte Chemie - International Edition* **2007**, *46*, 52–66.

16. Thirugnanasambandam, M.; Iniyan, S.; Goic, R. *Renewable and Sustainable Energy Reviews* **2010**, *14*, 312–322.

17. Tian, Y.; Zhao, C. Y. *Applied Energy* **2013**, *104*, 538–553.

18. IEA International Energy Agency, *Technology Roadmap - Energy storage*; 2014.

19. IEA International Energy Agency, *Perspectives for the energy transition: the role of energy efficiency*; 2018.

20. Moth-Poulsen, K.; Ćoso, D.; Börjesson, K.; Vinokurov, N.; Meier, S. K.; Majumdar, A.; Vollhardt, K. P. C.; Segalman, R. A. *Energy & Environmental Science* **2012**, *5*, 8534–8537.

21. Kolpak, A. M.; Grossman, J. C. *Nano Letters* **2011**, *11*, 3156–3162.

22. Moth-Poulsen, K.; Brøndsted Nielsen), . E. M. *Organic Synthesis and Molecular Engineering*; 2014; pp 179–196.

23. Yoshida, Z.-I. *Journal of photochemistry* **1985**, *29*, 27–40.

24. Lennartson, A.; Roffey, A.; Moth-Poulsen, K. *Tetrahedron Letters* **2015**, *56*, 1457–1465.

25. Kucharski, T. J.; Tian, Y.; Akbulatov, S.; Boulatov, R. *Energy & Environmental Science* **2011**, *4*, 4449–4472.

26. Börjesson, K.; Lennartson, A.; Moth-Poulsen, K. *ACS Sustainable Chemistry & Engineering* **2013**, *1*, 585–590.

27. Jones, G.; Reinhardt, T.; Bergmark, W. *Solar Energy* **1978**, *20*, 241.

28. Bastianelli, C.; Caia, V.; Cum, G.; Gallo, R.; Mancini, V. *Journal of the Chemical Society, Perkin Transactions 2* **1991**, *35*, 679.

29. Kolpak, A. M.; Grossman, J. C. *The Journal of Chemical physicshemical physics* **2013**, *138*, 034303.

30. Durgun, E.; Grossman, J. C. *The Journal of Physical Chemistry Letters* **2013**, *4*, 854–860.

31. Boese, R.; Cammack, J. K.; Matzger, A. J.; Pflug, K.; Tolman, W. B.; Vollhardt, K. P. C.; Weidman, T. W. *Journal of the American Chemical Society* **1997**, *119*, 6757–6773.

32. Börjesson, K. et al. *Chemistry - A European Journal* **2014**, *20*, 15587–15604.

33. Blanco-Lomas, M.; Martínez-López, D.; Campos, P. J.; Sampedro, D. *Tetrahedron Letters* **2014**, *55*, 3361–3364.

34. Gurke, J.; Quick, M.; Ernsting, N. P.; Hecht, S. *Chem. Commun.* **2017**, *53*, 2150–2153.

35. Yang, N. C.; Shold, D. M.; Kim, B. *Journal of the American Chemical Society* **1976**, *98*, 6587–6596.

36. Cum, G.; Gallo, R.; Pitoni, E. *Tetrahedron Letters* **1983**, *24*, 3903–3904.

37. Bastianelli, C.; Caia, V.; Cum, G.; Gallo, R.; Mancini, V. *J. Chem. Soc. Perkin Trans* **1991**, 679–683.

38. Dong, L.; Feng, Y.; Wang, L.; Feng, W. *Chemical Society Reviews* **2018**, *47*, 7339–7368.

39. Gunnlaugsson, T.; Leonard, J. P.; Murray, N. S. *Organic Letters* **2004**, *6*, 1557–1560.

40. Qin, C.; Feng, Y.; Luo, W.; Cao, C.; Hu, W.; Feng, W. *Journal of Materials Chemistry A* **2015**, *3*, 16453–16460.

41. Åstrand, P.-O.; Ramanujam, P. S.; Hvilsted, S.; Bak, K. L.; Sauer, S. P. A. *J. Am. Chem. Soc.* **2000**, *122*, 3482–3487.

42. Taoda, H.; Hayakawa, K.; Kawase, K.; Yamakita, H. *J. Chem. Eng. Jpn.* **1987**, *20*, 265–270.

43. Feng, Y.; Liu, H.; Luo, W.; Liu, E.; Zhao, N.; Yoshino, K.; Feng, W. *Scientific Reports* **2013**, *3*, 3260.

44. Kucharski, T. J.; Ferralis, N.; Kolpak, A. M.; Zheng, J. O.; Nocera, D. G.; Grossman, J. C. *Nature chemistry* **2014**, *6*, 441–7.

45. Zhitomirsky, D.; Cho, E.; Grossman, J. C. *Advanced Energy Materials* **2016**, *6*, 1502006.

46. Cho, E. N.; Zhitomirsky, D.; Han, G. G. D.; Liu, Y.; Grossman, J. C. *ACS Applied Materials & Interfaces* **2017**, *9*, 8679–8687.

47. Han, G. G. D.; Li, H.; Grossman, J. C. *Nature Communications* **2017**, *8*, 1446.

48. Cacciarini, M.; Skov, A. B.; Jevric, M.; Hansen, A. S.; Elm, J.; Kjaergaard, H. G.; Mikkelsen, K. V.; Brøndsted Nielsen, M. *Chemistry - A European Journal* **2015**, *21*, 7454–7461.

49. Cacciarini, M.; Jevric, M.; Elm, J.; Petersen, A. U.; Mikkelsen, K. V.; Nielsen, M. B. *RSC Advances* **2016**, *6*, 49003–49010.

50. Hansen, M. H.; Elm, J.; Olsen, S. T.; Gejl, A. N.; Storm, F. E.; Frandsen, B. N.; Skov, A. B.; Nielsen, M. B.; Kjaergaard, H. G.; Mikkelsen, K. V. *The Journal of Physical Chemistry A* **2016**, *120*, 9782–9793.

51. Kilde, M. D.; Arroyo, P. G.; Gertsen, A. S.; Mikkelsen, K. V.; Nielsen, M. B. *RSC Advances* **2018**, *8*, 6356–6364.

52. Torre-Pierna, H.; Roscini, C.; Vlasceanu, A.; Broman, S. L.; Jevric, M.; Cacciarini, M.; Nielsen, M. B. *Dyes and Pigments* **2017**, *145*, 359–364.

53. Vlasceanu, A.; Frandsen, B. N.; Skov, A. B.; Hansen, A. S.; Rasmussen, M. G.; Kjaergaard, H. G.; Mikkelsen, K. V.; Nielsen, M. B. *The Journal of Organic Chemistry* **2017**, *82*, 10398–10407.

54. Wang, Z.; Udmark, J.; Börjesson, K.; Rodrigues, R.; Roffey, A.; Abrahamsson, M.; Nielsen, B.; Moth-poulsen, K. *ChemSusChem* **2017**, *10*, 3049–3055.

55. Hammond, G. S.; Turro, N.; Fischer, A. *Journal Of The American Chemical Society* **1961**, *83*, 4674–4675.

56. Hammond, G. S.; Wyatt, P.; DeBoer, D. C.; Turro, N. J. *J. Am. Chem. Soc.* **1964**, *86*, 2532 – 2533.

57. Bren, V. A.; Dubonosov, A. D.; Minkin, V. I.; Chernoivanov, V. A. *Russian Chemical Reviews* **1991**, *60*, 913–948.

58. Hautala, R. R.; King, R. B.; Kutal, C. *Solar Energy - Chemical Conversion and Storage*; 1979.

59. Dubonosov, A. D.; Bren, V. A.; Minkin, V. I. *Organic Photochemistry and Photobiology*; 2004; pp 17.1 – 17.34.

60. Dubonosov, A. D.; Bren, V. A.; Chernoivanov, V. A. *Russian Chemical Reviews* **2002**, *71*, 917–927.

61. Dubonosov, A. D.; Galichev, S. V.; Chernoivanov, V. A.; Bren, V. A.; Minkin, V. I. *Russian Journal of Organic Chemistry* **2001**, *37*, 77–81.

62. An, X.; Xie, Y. *Thermochimica Acta* **1993**, *220*, 17–25.

63. Miki, S.; Asako, Y.; Yoshida, Z.-I. *Chemistry Letters* **1987**, 195–198.

64. Bren, V. A.; Minkin, V. I.; Dubonosov, A. D.; Chernoivanov, V. A.; Rybalkm, V. P.; Borodkin, G. S. *Molecular Crystals and Liquid Crystals Science and Technology. Section A. Molecular Crystals and Liquid Crystals* **1997**, *297*, 247–253.

65. Chernoivanov, V. A.; Dubonosov, A. D.; Bren, V. A.; Minkin, V. I.; Suslov, A. N.; Borodkin, G. S. *Molecular Crystals and Liquid Crystals Science and Technology. Section A. Molecular Crystals and Liquid Crystals* **1997**, *297*, 239–245.

66. Minkin, V. I.; Breit, V. A.; Cherwoivanov, V. A.; Dubonosov, A. D.; Galichev, S. V. *Molecular Crystals and Liquid Crystals Science and Technology. Section A. Molecular Crystals and Liquid Crystals* **1994**, *246*, 151–154.

67. Miki, S.; Maruyama, T.; Ohno, T.; Tohma, T.; Toyama, S.-I.; Yoshida, Z.-I. *Chemistry Letters* **1988**, *17*, 861–864.

68. Toda, T.; Hasedawa, E.; Mukai, T.; Tsuruta, H.; Hagiwara, T.; Yoshida, T. *Chemistry Letters* **1982**, 1551–1554.

69. Jack, K.; Machin, B.; Tigchelaar, A.; Tam, W. *Curr. Org. Synth.* **2013**, *10*, 584–630.

70. Nagai, T.; Shimada, M.; Ono, Y.; Nishikubo, T. *Macromolecules* **2003**, *36*, 1786–1792.

71. Laine, P.; Launay, J.-P.; Argazzi, R.; Bignozzi, C.-A. *Inorganic Chemistry* **1996**, *35*, 711–714.

72. Basu, A.; Saple, A. R.; Sapre, N. Y. *Journal of the Chemical Society, Dalton Transactions* **1987**, 1797.

73. Franceschi, F.; Guardigli, M.; Solari, E.; Floriani, C.; Chiesi-Villa, A.; Rizzoli, C. *Inorganic Chemistry* **1997**, *36*, 4099–4107.

74. Maruyama, K.; Tamiaki, H. *Journal of Organometallic Chemistry* **1986**, *51*, 602.

75. Philippopoulos, C.; Economou, D.; Constantine, E.; Marangozis, J. *Industrial & Engineering Chemistry Product Research and Development* **1983**, *22*, 627–633.

76. Oueslati, A.; Ben Romdhane, H.; Martin, V.; Schiets, F.; Mercier, R.; Chaãbouni, R. *Journal of Polymer Science, Part A: Polymer Chemistry* **2011**, *49*, 1988–1998.

77. Kamogawa, H.; Yamada, M. *Macromolecules* **1988**, *21*, 918–923.

78. Nishikubo, T.; Kameyama, A.; Kishi, K.; Kawashima, T.; Fujiwara, T.; Hijikata, C. *Macromolecules* **1992**, *25*, 4469–4475.

79. Tranmer, G. K.; Tam, W. *Synthesis* **2002**, *2002*, 1675–1682.

80. Yoo, W. J.; Tsui, G. C.; Tam, W. *European Journal of Organic Chemistry* **2005**, 1044–1051.

81. Gray, V.; Lennartson, A.; Ratanalert, P.; Börjesson, K.; Moth-Poulsen, K. *Chemical Communications* **2014**, *50*, 5330–5332.

82. Quant, M.; Lennartson, A.; Dreos, A.; Kuisma, M.; Erhart, P.; Börjesson, K.; Moth-poulsen, K. *Chem. Eur. J.* **2016**, *22*, 13265 – 13274.

83. Kuisma, M.; Lundin, A.; Moth-Poulsen, K.; Hyldgaard, P.; Erhart, P. *ChemSusChem* **2016**, *9*, 1786–1794.

84. Kuisma, M. J.; Lundin, A. M.; Moth-Poulsen, K.; Hyldgaard, P.; Erhart, P. *Journal of Physical Chemistry C* **2016**, *120*, 3635–3645.

85. Plate, A. F.; Pryanishnikova, M. A. *Bulletin of the Academy of Sciences of the USSR, Division of Chemical Science* **1956**, *5*, 753–754.

86. Spivack, K. J.; Walker, J. V.; Sanford, M. J.; Rupert, B. R.; Ehle, A. R.; Tocyloski, J. M.; Jahn, A. N.; Shaak, L. M.; Obianyo, O.; Usher, K. M.; Goodson, F. E. *The Journal of Organic Chemistry* **2017**, *82*, 1301–1315.

87. DePuy, C. H.; Ponder, B. W.; Fitzpatrick, J. D. *Angewandte Chemie - International Edition* **1962**, *1*, 404.

88. Lucchi, O. D.; Modena, G. *Tetrahedron* **1984**, *40*, 2585–2632.

89. Singh, V. K.; Deota, P. T.; Raju, B. N. S. *Synthetic Communications* **1987**, *17*, 593–599.

90. Magnusson, G. *Journal of Organic Chemistry* **1985**, *50*, 1998–1998.

91. Holder, R. W.; Daub, J. P.; Baker, W. E.; Gilbert, R. H.; Graf, N. A. *Journal of Organic Chemistry* **1982**, *47*, 1445–1451.

92. Baldwin, J. E.; Ghatlia, N. D. *Journal of the American Chemical Society* **1989**, *111*, 3319–3325.

93. Dyachenko, A. I.; Menchikov, L. G.; Nefedov, O. M. *Bulletin of the Academy of Sciences of the USSR, Division of Chemical Science* **1984**, *33*, 1526–1527.

94. Zenova, A. Y.; Borisenko, A. A.; Platonov, V.; Proskurnina, M. V.; Zefirov, N. S. *Russian Journal of Organic Chemistry* **1996**, *32*, 951 – 954.

95. Singh, R. P.; Cao, G.; Kirchmeier, R. L.; Shreeve, J. M. *Journal of Organic Chemistry* **1999**, *64*, 2873–2876.

96. Jorner, K.; Dreos, A.; Emanuelsson, R.; Ouissam, E. B.; Fdez Galvan, I.; Börjesson, K.; Feixas, F.; Lindh, R.; Burkhard, Z.; Moth-Poulsen, K.; Ottosson, H. *Journal of Materials Chemistry A* **2017**, *5*, 12369–12378.

97. Nagai, T.; Fujii, K.; Takahashi, I.; Shimada, M. *Bull. Chem. Soc. Jpn,* **2001**, *74*, 1673–1677.

98. Koblik, A. V.; Murad'yan, L. A.; Dubonosov, A. D.; Zolotovskova, G. P. *Chemistry of Heterocyclic Compounds* **1990**, *26*, 259–263.

99. Tebikachew, B. E.; Edhborg, F.; Kann, N.; Albinsson, B.; Moth-Poulsen, K. *Physical Chemistry Chemical Physics* **2018**, *20*.

100. Ikezawa, H.; Kutal, C.; Yasufuku, K.; Yamazaki, H. *J. Am. Chem. Soc.* **1986**, *108*, 1589–1594.

101. Haynes, W. M. *CRC Handbook of Chemistry and Physics; a Ready-Reference Book of Chemical and Physical Data, 92d ed.*; 2011.

102. Panasonic, https://news.panasonic.com/jp/press/data/jn091225-1/jn091225-1.html. 2009.

103. Dreos, A.; Wang, Z.; Udmark, J.; Ström, A.; Erhart, P.; Börjesson, K.; Nielsen, M. B.; Moth-Poulsen, K. *Advanced Energy Materials* **2018**, *8*, 1–9.

104. Kabakoff, D. S.; Buenzli, J.-C. G.; Oth, J. F. M.; Hammond, W. B.; Berson, J. A. *J. Am. Chem. Soc.* **1975**, *97*, 1510.

105. Jevric, M.; Petersen, A. U.; Mansø, M.; Singh, S. K.; Wang, Z.; Dreos, A.; Sumby, C.; Nielsen, M. B.; Börjesson, K.; Erhart, P.; Moth-Poulsen, K. *Chemistry - A European Journal* **2018**, *24*, 12767–12772.

106. Eyring, H. *J. Chem. Phys.* **1935**, *3*, 107–115.

107. Evans, M. G.; Polanyi, M. *Trans. Faraday Soc.* **1935**, *31*, 875–894.

108. Börjesson, K.; Dzebo, D.; Albinsson, B.; Moth-Poulsen, K. *Journal of Materials Chemistry A* **2013**, *1*, 8499–8680.

109. Wang, Z.; Roffey, A.; Losantos, R.; Lennartson, A.; Jevric, M.; Petersen, A. U.; Quant, M.; Dreos, A.; Wen, X.; Sampedro, D.; Börjesson, K.; Moth-poulsen, K. *Energy & Environmental Science* **2019**, *12*, 187–193.

110. Tebikachew, B. E.; Li, H. B.; Pirrotta, A.; Börjesson, K.; Solomon, G. C.; Hihath, J.; Moth-Poulsen, K. *Journal of Physical Chemistry C* **2017**, *121*, 7094–7100.

111. Morino, S.; Watanabe, W.; Magaya, Y.; Yamashita, T.; Horie, K.; Nishikubo, T. *Journal of Photopolymer Science and Technology* **1994**, *7*, 121–126.

112. Takahashi, S.; Samata, K.; Muta, H.; Machida, S. *Applied Physics Letters* **2001**, *78*, 13–15.

113. Nishino, H.; Inoue, Y. Chiral norbornadiene-quadricyclane derivative and reversible optical recording material using it. JKXXAF; JP2000086588. 2000.

114. Starck, F.; Jones, P. G.; Herges, R. *European Journal of Organic Chemistry 1998*, 2533–2539.

115. De Silva, P. A.; Gunaratne, N. H.; McCoy, C. P. *Nature* **1993**, *364*, 42–44.

116. Pilarczyk, K.; Wlaźlak, E.; Przyczyna, D.; Blachecki, A.; Podborska, A.; Anathasiou, V.; Konkoli, Z.; Szaciłowski, K. *Coordination Chemistry Reviews* **2018**, *365*, 23–40.

117. Andréasson, J.; Pischel, U. *Chem. Soc. Rev.* **2015**, *44*, 1053–1069.

118. Erbas-cakmak, S.; Kolemen, S.; Gunnlaugsson, T.; James, T. D.; Akkaya, E. U.; Sedgwick, A. C. *Chemical Society Reviews* **2018**,

119. Balzani, V.; Credi, A.; Venturi, M. *ChemSusChem*; 2008; Vol. 1; pp 26–58.

120. Magri, D. C.; Camilleri Fava, M.; Mallia, C. J. *Chem. Commun.* **2014**, *50*, 1009–1011.

121. Andréasson, J.; Straight, S. D.; Moore, T. A.; Moore, A. L.; Gust, D. *Chemistry - A European Journal* **2009**, *15*, 3936–3939.

122. Andréasson, J.; Pischel, U.; Straight, S. D.; Moore, T. A.; Moore, A. L.; Gust, D. *Journal of the American Chemical Society* **2011**, *133*, 11641–11648.

123. Angelos, S.; Khashab, N. M.; Yang, Y.-W.; Trabolsi, A.; Khatib, H. A.; Stoddart, J. F.; Zink, J. I. *Journal of the American Chemical Society* **2009**, *131*, 12912–12914, PMID: 19705840.

124. Erbas-Cakmak, S.; Akkaya, E. U. *Angewandte Chemie International Edition 52*, 11364–11368.

125. Erbas-Cakmak, S.; Bozdemir, O. A.; Cakmak, Y.; Akkaya, E. U. *Chem. Sci.* **2013**, *4*, 858–862.

126. Andréasson, J.; Pischel, U. *Chem. Soc. Rev.* **2018**, *47*, 2266–2279.

127. Lustgarten, O.; Motiei, L.; Margulies, D. *ChemPhysChem* **2017**, *18*, 1678–1687.

128. Margulies, D.; Felder, C. E.; Melman, G.; Shanzer, A. *Journal of the American Chemical Society* **2007**, *129*, 347–354.

129. Kumar, S.; Luxami, V.; Saini, R.; Kaur, D. *Chemical Communications* **2009**, *0*, 3044–3046.

130. Sun, W.; Zhou, C.; Xu, C. H.; Fang, C. J.; Zhang, C.; Li, Z. X.; Yan, C. H. *Chemistry - A European Journal* **2008**, *14*, 6342–6351.

131. Kink, F.; Collado, M. P.; Wiedbrauk, S.; Mayer, P.; Dube, H. *Chemistry - A European Journal* **2017**, *23*, 6237–6243.

132. Zhu, J.; Yang, X.; Zhang, L.; Zhang, L.; Lou, B.; Dong, S.; Wang, E. *Chemical Communications* **2013**, *49*, 5459–5461.

133. Jiang, X. J.; Ng, D. K. *Angewandte Chemie - International Edition* **2014**, *53*, 10481–10484.

134. Stranius, K.; Börjesson, K. *Scientific Reports* **2017**, *7*, 41145.

135. Hatchard, C. G.; Parker, C. A. *Proceedings of the Royal Society of London A: Mathematical, Physical and Engineering Sciences* **1956**, *235*, 518–536.

136. Casarini, D.; Lunazzi, L.; Mazzanti, A. *European Journal of Organic Chemistry* **2010**, *2*, 2035–2056.